

1 **Title:** Sensitivity of potential evapotranspiration to changes in climate variables for different Australian climatic
2 zones

3 **Author names and affiliations:** Danlu Guo^a; Seth Westra^a; Holger R. Maier^a.

4 ^a School of Civil, Environmental and Mining Engineering, the University of Adelaide, North Terrace, Adelaide SA
5 5005, Australia.

6 **Corresponding author:** Danlu.Guo@Adelaide.edu.au

7 **Permanent address:** School of Civil, Environmental and Mining Engineering, the University of Adelaide, North
8 Terrace, Adelaide SA 5005, Australia.

9 **Abstract**

10 Understanding the factors that have an impact on the sensitivity of potential evapotranspiration (PET) to
11 changes in different climate variables is critical to assessing the possible implications of anthropogenic climate
12 change on the catchment water balance. Using a global sensitivity analysis, this study assessed the implications
13 of baseline climate conditions on the sensitivity of PET to a large range of plausible changes in temperature (T),
14 relative humidity (RH), solar radiation (R_s) and wind speed (u_z). The analysis was conducted at 30 Australian
15 locations representing different climatic zones, using the Penman-Monteith and Priestley-Taylor PET models.
16 Results from both models suggest that the baseline climate can have a substantial impact on overall PET
17 sensitivity. In particular, approximately two-fold greater changes in PET were observed in cool-climate energy-
18 limited locations compared to other locations in Australia, indicating the potential for elevated water loss as a
19 result of increasing actual evapotranspiration (AET) in these locations. The two PET models consistently
20 indicated temperature to be the most important variable for PET, but showed large differences in the relative
21 importance of the remaining climate variables. In particular, for the Penman-Monteith model wind and relative
22 humidity were the second-most important variable for dry and humid catchments, respectively, whereas for the
23 Priestley-Taylor model solar radiation was the second-most important variable, particularly for warmer
24 catchments. This information can be useful to inform the selection of suitable PET models to estimate future
25 PET for different climate conditions, providing evidence on both the structural plausibility and input uncertainty
26 for the alternative models.

27 **Keywords:** climate impact assessment; evapotranspiration; climate zones; Penman-Monteith; Priestley-Taylor;
28 global sensitivity analysis

29

30 1. Introduction

31 Evapotranspiration (ET) is critical in assessing the impacts of anthropogenic climate change on the catchment
32 water balance, with ET fluxes accounting for about 62% of land-surface precipitation on average globally
33 (Dingman, 2015) and thus representing the dominant loss of water from a large proportion of catchments
34 worldwide. ET fluxes are affected by climate change through a cascade of processes that begins with the
35 increasing concentration of greenhouse gases, as well as their attendant impacts on large-scale circulation and
36 associated changes to the global distribution of energy and moisture. These large-scale processes lead to local-
37 scale changes in the atmosphere, which in turn influence the catchment water balance through a set of
38 terrestrial hydrological processes by which precipitation is converted into actual ET (AET), runoff and
39 groundwater recharge (Oudin et al., 2005).

40 Climate impact studies that investigate the influence of climate forcings on the catchment water balance are
41 usually based on projections of future climate represented by climate variables such as temperature and solar
42 radiation from general circulation models (GCMs), which are converted into potential ET (PET) using one or
43 several PET models. The PET projections are combined with GCM projections of precipitation (P), which
44 together can be used to directly estimate the water deficit (Taylor et al., 2013; Chang et al., 2016). Alternatively,
45 rainfall-runoff models can be used to translate the changes in P and PET into changes in runoff (e.g. Akhtar et al.,
46 2008; Chiew et al., 2009; Koedyk and Kingston, 2016), as well as associated information such as the impact on
47 catchment yield (Wilby et al., 2006), water supply security (Paton et al., 2014, 2013) and flood risk (Bell et al.,
48 2016). Therefore, to quantify the specific impact of changes in ET on the water balance, a good understanding
49 of the sensitivity of PET to potential changes in its key influencing climatic variables is required (Goyal,
50 2004; Tabari and Hosseinzadeh Talaei, 2014). This is particularly relevant given the recent focus on ‘scenario-

51 neutral' (or 'bottom-up') approaches to climate impact assessment (Brown et al., 2012;Prudhomme et al.,
52 2010;Culley et al., 2016), which require the sensitivity of a given system to potential changes in climate forcings
53 to be estimated (Prudhomme et al., 2013a;Steinschneider and Brown, 2013;Prudhomme et al., 2013b;Kay et al.,
54 2014;Guo et al., 2016a).

55 Furthermore, the sensitivity of PET can provide critical evidence in relation to which models are most
56 appropriate for PET estimation under climate change conditions, which is particularly relevant to the ongoing
57 debate on the potential trade-off between model complexity and reliability. Complex models such as the
58 Penman-Monteith model are often recommended for their ability to better represent the physical processes
59 that affect PET (McVicar et al., 2012;Donohue et al., 2010;Barella-Ortiz et al., 2013). For example, the Penman-
60 Monteith model can account for the effects of wind, and thus can assist to explain at least part of the observed
61 decreases in pan evaporation with increases in temperature in many locations globally – the 'evaporation
62 paradox' – as due to the observed decreases in wind speed (Roderick et al., 2007;McVicar et al., 2008;Lu et al.,
63 2016). However, simpler empirical models may also be preferable under some conditions, as they require a
64 smaller number of input climate variables, which might be able to be projected with greater confidence with
65 GCMs, and thus leading to greater confidence in the corresponding PET estimates (Kay and Davies,
66 2008;Ekström et al., 2007;Ravazzani et al., 2014). For example, there is reasonable confidence in projections of
67 temperature and relative humidity in Australia for a given emission scenario, but less confidence in projections
68 of wind due to sub-grid effects of orography and other land-surface features (Flato et al., 2013;CSIRO and
69 Bureau of Meteorology, 2015). In these situations, models such as the Priestley-Taylor model that do not
70 depend on wind may produce more reliable estimates of PET compared to the more complex Penman-Monteith
71 model. Thus, the choice of climate variables to include in climate impact assessments must be informed both by

72 the relative importance of each variable on projections of PET (e.g. Tabari and Hosseinzadeh Talaei, 2014), and
73 the likely confidence in the projections of each variable (e.g. Flato et al., 2013; Johnson and Sharma, 2009).

74 Sensitivity analysis methods have been employed in a number of recent studies to assess the overall sensitivity
75 of PET estimated by the Penman-Monteith model to potential changes in climate, as well as to better
76 understand the relative importance of different climate variables on overall PET sensitivity. For example, Goyal
77 (2004) found that PET was most sensitive to perturbations in temperature, followed by solar radiation, wind
78 speed and vapor pressure, at a single study site in an arid region in India. Tabari and Hosseinzadeh Talaei (2014)
79 also looked at the sensitivity of PET to perturbations of historical climate data from eight meteorological
80 stations representing four climate types in Iran, and concluded that the importance of wind speed and air
81 temperature was lower while that of sunshine hours was higher for a humid location compared to an arid
82 location. Gong et al. (2006) found that the differences in PET sensitivity across the upper, middle and lower
83 regions of the Changjiang (Yangtze) basin in China were largely due to contrasting baseline wind speed patterns.
84 However, most of these PET sensitivity analysis studies focused on a limited number of study sites and/or
85 climatic zones, so that the specific causes for varying PET sensitivity at different locations, such as the roles of
86 climatic and hydrological conditions, remain unclear. Consequently, it is difficult to extrapolate our existing
87 knowledge of PET sensitivity and the relative importance of each climate variable to new locations, which is
88 essential for assessing the water balance at regional scales.

89 To address the shortcomings of existing studies outlined above, this study aims to gain an understanding of (i)
90 the sensitivity of PET estimates to changes in the key climatic variables which influence PET, and how these
91 sensitivity estimates are affected by varying baseline hydrologic and climatic conditions at different locations;
92 and (ii) the relative importance of these climatic variables for PET, and how this changes with the baseline

93 hydrologic and climatic conditions at different locations. These aims were achieved by analyzing the sensitivity
94 of PET to perturbations in four of its driving climatic variables, namely temperature (T), relative humidity (RH),
95 solar radiation (R_s) and wind speed (u_z), at 30 study sites across Australia representing a range of climate zones.
96 Both the Penman-Monteith and Priestley-Taylor models were used, as they represent different
97 conceptualizations of the PET-related processes, with both models being widely used for climate impact
98 assessments (Felix et al., 2013; Arnell, 1999; Gosling et al., 2011; Kay et al., 2009; Prudhomme and Williamson,
99 2013; Donohue et al., 2009). It is worth noting that the potential changes in one climate variable can be
100 amplified or offset by changes in another variable (for examples see the discussions of 'evaporation paradox' in
101 Lu et al., 2016; Roderick and Farquhar, 2002), which can affect the relative importance of each variable. To
102 account for this effect, a global sensitivity analysis method was used, with similar methods being applied to
103 account for the impact of joint variations in the input variables on the output from a variety of environmental
104 models, ranging from conceptual rainfall-runoff models (e.g. Tang et al., 2007a; Tang et al., 2007c) to complex
105 models which consider a number of surface-groundwater processes (e.g. Guillevic et al., 2002; van Griensven et
106 al., 2006; Nossent et al., 2011). The results of the global sensitivity analysis in this study were presented in terms
107 of both absolute sensitivity of PET and relative sensitivity indices of each climate variable, and were used to
108 elucidate the specific roles of varying baseline hydro-climatic conditions on influencing these sensitivity
109 measures.

110 The subsequent sections of this paper are structured as follows. Section 2 introduces the data obtained from
111 the 30 study sites required for the global sensitivity analysis. Section 3 describes the approach to the global
112 sensitivity analysis of PET. Section 4 presents and discusses two sets of results which address the two study aims
113 respectively, as: (i) the estimated PET sensitivity to potential changes in temperature, solar radiation, humidity

114 and wind, and how this changes with location; and (ii) the relative importance of the four climate variables for
115 estimating PET, and how this changes with location. The study is summarized and concluded in Sect. 5.

116 2. Data

117 To represent contrasting hydro-climatic conditions for assessing PET sensitivity, we selected case study
118 locations within different Köppen classes in Australia. The original Köppen climate classification (Köppen et al.,
119 1930;Köppen, 1931) provides a useful categorization of hydro-climatic conditions at specific locations, which is
120 based on the long-term average levels and seasonal patterns of climatic and hydrologic variables, including
121 temperature, relative humidity and rainfall. A ‘modified Köppen classification’ system has been adapted for
122 Australia (as in Stern et al., 2000) and is now widely used in climatic and hydrologic studies to identify and
123 categorize case study locations (e.g. Johnson and Sharma, 2009;Rustomji et al., 2009;Li et al., 2014).

124 As mentioned in the Introduction, both the Penman-Monteith and the Priestley-Taylor models were used to
125 estimate PET for the global sensitivity analyses. The estimation of PET with these models relies on temperature,
126 relative humidity, solar radiation and (for the Penman-Monteith model only) wind speed. In addition, the
127 rainfall data were also obtained to assess the aridity of the different locations. We limited the selection of study
128 sites to those with 10 or more years of continuous climate data with no more than 5 % missing records over the
129 study period. This led to a final selection of 30 weather stations (Fig. 1), with a consistent data period from 1
130 January 1995 to 31 December 2004. The data obtained at each site are detailed as below:

- 131 • **Daily maximum and minimum temperature (T in °C), maximum and minimum relative humidity (RH
132 in %) and wind speed (u_z in $m\ s^{-1}$):** Data for each of these variables were obtained directly from each
133 weather station.

- **Daily solar radiation (R_s in $\text{MJ m}^{-2} \text{ day}^{-1}$):** Daily solar radiation was calculated from daily sunshine hour data (n in h) obtained from each weather station, using the Ångström-Prescott equation as in McMahon et al. (2013).
- **Daily rainfall (mm):** Daily rainfall data were obtained from a rain gauge at each weather station.

Figure 1: Locations of 30 Australian weather stations (see Table 1 for the full names of these weather stations) selected for analysis, with reference to their corresponding climate classes derived following the modified Köppen classification (reproduced with data from Stern et al., 2000).

Table 1 shows the average values of the four PET-related climate variables, as well as the rainfall within the study period, at each of the 30 sites. As can be seen, there are large differences in the average values of each variable, highlighting large differences in the climatic conditions across the 30 sites. In addition, a quantity particularly relevant to ET processes is the long-term averaged ratio of PET to precipitation (PET/P), which describes whether a location is water-limited ($\text{PET/P} > 1$) or energy-limited ($\text{PET/P} < 1$) (Gerrits et al., 2009; McVicar et al., 2010). This ratio was estimated for each site and is also shown in Table 1 (with the point colour in Fig. 1 indicating whether the location is water-limited or energy-limited). The range of PET/P values indicates substantial variations in the water availability conditions at different study sites. Note that these ratios were based on the estimates of PET from the Penman-Monteith model. Although the use of Priestley-Taylor model resulted in different PET estimates at each site, the categorization of water- and energy-limited catchments was generally consistent with those from Penman-Monteith, with different categories only shown at four out of the 30 study sites (sites 6, 19, 20 and 27).

Table 1: Names, locations and average climate conditions of the 30 weather stations over the study period (1995-2004).

157 3. Method

158 3.1. Overview

159 A schematic of the approach followed in study is shown in Fig. 2. As a required model input for the global
160 sensitivity analysis, a large number of representative samples were first obtained for the four climate variables
161 which influence PET (T , RH , R_s and u_2) at each study site, by perturbing the corresponding historical climate data
162 (Sect. 3.2). The outputs of the global sensitivity analysis (i.e. the responses of PET) were estimated with the
163 Penman-Monteith and Priestley-Taylor models (Sect. 3.3). To understand the PET sensitivity and the relative
164 importance of the four climate variables in influencing PET and how these change with location, a global
165 sensitivity analysis was conducted with the responses of PET to the climate perturbations (Sect. 3.4). This
166 proceeded in two parts:

- 167 (1) To assess the sensitivity of PET to the climate variables, the percentage changes in PET in response to all
168 the climate perturbations were estimated relative to the baseline PET at each location. To observe the
169 impact of varying baseline hydro-climatic conditions, the sensitivity obtained from each PET model was
170 also plotted against the baseline levels of each climate variable for all study sites.
- 171 (2) To assess the relative importance of each climate variable, the PET sensitivity to all climate
172 perturbations in (1) was first compared to the conditional sensitivity when holding each variable
173 constant. This comparison enables an assessment of the relative impact of each variable on the total
174 PET sensitivity. An alternative presentation of the individual and interaction effects of the climate
175 variables was achieved using the Sobol' method (Sobol' et al., 2007). Here, the total variance of PET was

176 estimated based on different samples drawn from the perturbed ranges of each climate variable, and
177 then partitioned into the individual contribution from each climate variable and their interactions (see
178 Appendix A.1. for details). The Sobol' first-order sensitivity indices were estimated and plotted against
179 the baseline levels of each climate variable for all study sites to explore the role of varying baseline
180 hydro-climatic conditions on the relative importance of each climatic variable for PET.

181 **Figure 2: Schematic of the method used in this study.**
182

183 3.2. Representing plausible changes in the climatic variables

184 As part of the global sensitivity analysis, a large number of representative combinations of the changes in the
185 four climate variables (T , RH , R_s and u_2) were obtained. The upper and lower bounds for perturbing each climate
186 variable were determined based on the uncertainty bounds of projections for 2100 for Australia (Stocker et al.,
187 2013). The selected bounds are given in Table 2, which are all slightly wider than those presented in Stocker et
188 al. (2013) to encompass a comprehensive range of plausible future climate change scenarios. Within these
189 bounds, samples were drawn for different combinations of changes in each climatic variable. Latin hypercube
190 sampling (LHS) was used for this purpose due to its effectiveness in covering multi-dimensional input spaces
191 (Osiede and Beck, 2001;Sieber and Uhlenbrook, 2005;Tang et al., 2007b).

192 **Table 2: Plausible perturbation bounds for each climate variable relative to their current levels.**
193

194 According to Nossent et al. (2011) and Zhang et al. (2015), the sample size was selected to ensure the
195 convergence of the first- and total-order Sobol' sensitivity indices, which occurs when the width of the 95 %
196 confidence intervals from 1000-fold bootstrap resampling of the each index is below 10 % of the corresponding

197 mean obtained from bootstrapping. Specifically, we generated different sizes of LHS samples of climate
198 perturbations with the historical climate data from one study site, from which the PET responses were
199 estimated using the Penman-Monteith model. The 1000-fold bootstrap estimates for the Sobol' first- and total-
200 order sensitivity indices for each climate variable were then derived (as in Eqn. 1.2 and 1.5 in Appendix A.1.,
201 respectively) for each sample size. It was observed that both the Sobol' indices began to converge when the
202 sample size exceeded 5000, and this was therefore used as the LHS sample size for all the sensitivity
203 experiments in this study. Based on this sample size, a total of 30000 Sobol' samples were compiled as required
204 to estimate the first- and total-order indices (as detailed in Appendix A.1.), which correspond to 30000 climate
205 perturbations to be used to test PET sensitivity.

206 To generate time series of perturbed climate data, the 30000 joint perturbations to the four climate variables
207 obtained by LHS were treated as change factors, and applied to the time series of daily values of the
208 corresponding historical data. Rather than using a single daily mean value of temperature and relative humidity,
209 the two PET models used in this study require both the daily minimum and maximum values; therefore each
210 pair of temperature variables and relative humidity variables was considered jointly and thus perturbed by the
211 same amount for each day. In addition, to ensure physical plausibility of the perturbations, the daily maximum
212 and minimum values of relative humidity were capped at a maximum of 100%.

213 3.3. Estimating PET responses to climate perturbation

214 To represent the responses in PET as a result of the climate perturbations, we used both the Penman-Monteith
215 and Priestley-Taylor models, which provide contrasting process representations to estimate PET. The Penman-
216 Monteith model is often referred to as a combinational model, as it combines the energy balance and mass
217 transfer components of ET, and takes into account vegetation-dependent processes such as aerodynamic and

218 surface resistances (Eqn. 2.1 in Appendix A.2.). The model requires input of six climate variables, namely, T_{\max} ,
219 T_{\min} , RH_{\max} , RH_{\min} , R_s and u_z . The Priestley-Taylor model consists of a simpler structure, considering only the
220 energy balance, without consideration of mass transfer or any impact from vegetation (Eqn. 3.1 in Appendix
221 A.3.). Therefore, the Priestley-Taylor model is also referred to as a radiation-based model. The model only
222 requires five climate variables, including T_{\max} , T_{\min} , RH_{\max} , RH_{\min} and R_s .

223 To minimize the potential confounding effects of differences in vegetated surface, the evaporative surface was
224 assumed to be reference crop for all study sites, so that it was possible to use the FAO-56 version of the
225 Penman-Monteith model (Allen et al., 1998). The detailed formulations of the two PET models, as well as the
226 relevant constants and assumptions, are included in McMahon et al. (2013). Both models were implemented
227 using the R package *Evapotranspiration* (<http://cran.r-project.org/web/packages/Evapotranspiration/index.html>)
228 (Guo et al., 2016b). From each model, two sets of estimated PET were obtained: (i) a single set of baseline
229 (historical) PET data at each study site with the historical climate data; (ii) 30000 sets of perturbed PET data at
230 each study site corresponding to the 30000 sets of perturbed climate data obtained using LHS, as detailed in
231 Sect. 3.2.

232 3.4. Analyses of PET sensitivity

233 To assess the overall sensitivity of PET to plausible climate change, we first estimated the annual average
234 percentage changes in PET (relative to the baseline PET) using all climate perturbations at the 30 study sites,
235 with estimates from both the Penmen-Monteith and Priestley-Taylor models. A closer investigation of how PET
236 sensitivity varies with baseline climate was conducted by plotting all monthly PET responses against the average
237 levels of each climate variable, for all study sites and all months. The reason for the choice of monthly timescale

238 is that for some study sites, the climate can vary substantially by season, so that an annual analysis might
239 obscure important sub-annual effects.

240 To assess the relative importance of each climate variable for PET estimation from each model, we first
241 compared two sets of PET sensitivity, namely:

242 (1) The unconditional sensitivity of PET obtained from the entire 30000 sets of climate perturbations from
243 LHS; and

244 (2) The conditional sensitivity of PET assuming no changes in one of the climate variables, obtained using a
245 subset of all climate perturbations used in (1), for which the changes in the specific conditioning climate
246 variable were close to zero (within ± 0.1 °C for T , and within ± 0.1 % for the other three variables).

247 In this way any difference between (1) and (2) was purely contributed by the impact of changing the specific
248 conditioning climate variable. To quantify and compare the relative importance of each climate variable, we
249 then utilized the Sobol' method, which was implemented within the R package *sensitivity* ([https://cran.r-](https://cran.r-project.org/web/packages/sensitivity/index.html)
250 [project.org/web/packages/sensitivity/index.html](https://cran.r-project.org/web/packages/sensitivity/index.html)). We estimated the Sobol' first-order sensitivity indices (as in
251 Eqn. 1.2, Appendix A.1.) to assess the role of each individual climate variable for each PET model, at the 30
252 study sites. The sum of all interaction effects was also calculated for each location as the difference between
253 the sum of all first-order indices and one (Eqn. 1.6, Appendix A.1.). The Sobol' first-order indices were then
254 plotted against the baseline levels of each climate variable at the 30 study sites, to assess how the relative
255 importance changes with the baseline climatic conditions.

256 4. Results and discussion

257 4.1. Sensitivity of PET to potential climate change for different climate zones

258 We start by assessing the sensitivity of PET to the full set of climate perturbations at the 30 study sites at the
259 annual timescale, using both the Penman-Monteith and Priestley-Taylor models. The sensitivity results are
260 presented in Table 3 in terms of the minimum, maximum and average changes of PET relative to the 1995-2004
261 baseline based on the 30000 LHS replicates at each study site. The two models suggest similar average PET
262 sensitivity at most locations, with the sensitivity of the Penman-Monteith model averaged across all the
263 locations (+13.38 %) being slightly higher than that for the Priestley-Taylor model (+10.91 %). Greater
264 differences between the two models were observed when considering the ranges of sensitivity values. In
265 particular, the minimum and maximum values (averaged across all the 30 sites) were -13.66 % and +47.09 % for
266 the Penman-Monteith model, respectively, compared to -7.39 % and +34.47 % for the Priestley-Taylor model.
267 This corresponds to a range for the Penman-Monteith model being approximately 45 % wider than that of the
268 Priestley-Taylor model.

269 **Table 3: Annual average PET sensitivity to the full set of climate perturbations (as % changes to baseline PET) from**
270 **the Penman-Monteith and Priestley-Taylor models at the 30 study sites relative to the 1995-2004 baseline. The**
271 **maximum and minimum sensitivity values from each model are shaded in grey.**
272

273 For each PET model, the sensitivity values display substantial variation across the locations, with both models
274 suggesting the lowest PET sensitivity at arid locations and highest PET sensitivities at humid locations, as was
275 also observed in Table 3. Specifically, the Penman-Monteith model identified the highest average PET sensitivity

276 at Flinders Island (+17.15 %), with the lowest sensitivity at Alice Springs (+9.80 %). The Priestley-Taylor model
277 identified the highest average PET sensitivity at Hobart (+17.77 %), with the lowest at Tennant Creek (+7.09 %).

278 To further investigate how PET sensitivity varies with different climatic conditions, we now focus on the
279 associations between the PET sensitivity values and the baseline levels of the four climate variables for each
280 month of the year and across the 30 study sites. Starting with the Penman-Monteith model (Fig. 3), it is clear
281 that the PET sensitivity displays a clear association with the baseline levels of climate variables, with higher
282 sensitivity values for locations that are cooler (low T), more humid (high RH), and receiving less solar radiation
283 (low R_s). The highest associations can be found with T (Fig. 3a), with the monthly changes in PET ranging from -
284 30.2% to +98.3 % for the lowest baseline T value of 5.0 °C, compared to a range of -13.3 % to +46.6 % for the
285 highest baseline T of 30.3 °C. Similarly, the range of Penman-Monteith PET sensitivity values also shows clear
286 decreases with baseline R_s (Fig. 3c), and increases with baseline RH (Fig. 3b). The baseline u_z (Fig. 3d) levels
287 show no obvious impact on the PET sensitivity.

288 **Figure 3: Monthly PET responses from the Penman-Monteith model, plotted against the monthly baseline levels of (a)**
289 **temperature, (b) relative humidity, (c) solar radiation and (d) wind speed at 30 study sites. Each interval represents**
290 **the range of all PET responses to the full set of climate perturbations for a single month at a single location, with the**
291 **mean represented by the point on the line. The classification of energy- and water-limited months are based on the**
292 **corresponding monthly PET/P ratios.**

293

294 The sensitivity from Priestley-Taylor was also investigated (Fig. 4), and results are consistent with the results
295 from the Penman-Monteith model, although the overall ranges were lower for each variable as anticipated
296 from the results in Table 3. Interestingly, regardless of the choice of PET model, the range of sensitivity values at
297 the monthly scale is higher than the range for the annual scale suggesting greater uncertainty at higher
298 temporal resolutions.

299 **Figure 4: Monthly PET responses from the Priestley-Taylor model, plotted against the monthly baseline levels of (a)**
300 **temperature, (b) relative humidity, (c) solar radiation and (d) wind speed at 30 study sites. Each interval represents**
301 **the range of all PET responses to the full set of climate perturbations for a single month at a single location, with the**
302 **mean represented by the point on the line. The classification of energy- and water-limited months are based on the**
303 **corresponding monthly PET/P ratios.**
304

305 In addition to assessing the impact of baseline climatic conditions, we are also interested in the role of baseline
306 hydrological conditions (represented by the PET/P ratio at each study site) on PET sensitivity. Since the
307 hydrological conditions can vary substantially over the course of a year for each study site, for this analysis we
308 focused on the PET/P ratios estimated on a monthly basis, and thus differ from the long-term PET/P ratios
309 presented in Table 1. These results are also shown in Figs. 3 and 4, with red-colored bars denoting water-limited
310 conditions, and blue-colored bars denoting energy-limited conditions. These figures show that PET sensitivity is
311 generally larger under energy-limited conditions, regardless of the choice of PET model. In contrast, for water-
312 limited conditions, most sensitivity magnitudes only vary within approximately half of the entire range from
313 each PET model. However, when exploring the association with temperature (Figs. 3a and 4a) in more detail,
314 the sensitivity is in fact lowest for energy-limited conditions during warm months (i.e. when $T > 25$ °C,
315 corresponding to the monsoonal summer months in the northern parts of Australia), and highest for the
316 energy-limited conditions during cool months (i.e. when $T < 15$ °C, corresponding to the wet winter months in
317 southern Australia). This highlights that it is the atmospheric temperature, rather than the level of aridity, that
318 appears to affect the overall sensitivity. This finding leads to a different interpretation to previous studies,
319 which indicated that the dominant drivers of spatially varying PET include aridity (Tabari and Hosseinzadeh
320 Talaei, 2014) and wind speed (Gong et al., 2006).

321 The above results also have potential implications on likely AET changes in a future climate. In particular, the
322 above analysis shows that cool and humid regions and seasons appear to show the greatest sensitivity to PET,
323 and given that water is not expected to be limited for these cases, the ratio between AET and PET is also likely
324 to be the greatest for these cases. As such, one might expect a greater change to AET occurring at the locations
325 and during times of the year where PET is most sensitive to changes in climate.

326 As a potential limitation to the above analysis, some reliability issues of the Penman-Monteith model have been
327 discussed in a recent study by Milly and Dunne (2016), which suggested that the Penman-Monteith model may
328 overestimate the sensitivity in these energy-limited regions relative to a GCM-based AET benchmark. They
329 concluded that the potential changes in ET would be better described by GCMs than 'off-line' PET models (such
330 as the two models used in this study), as GCMs can explicitly consider more complex atmospheric processes,
331 such as the interaction between CO₂ and stomatal conductance. Nevertheless, it should be noted that the
332 current reliability of GCMs in simulating ET is also questionable, due to the uncertainty in representing soil
333 moisture and radiative energy at the evaporative surface (e.g. Seneviratne et al., 2013;Boé and Terray,
334 2008;Barella-Ortiz et al., 2013). In addition, due to the coarse scale of GCM output, downscaling is generally
335 required to post-process output for use at local and regional scales, which often adds further bias and
336 uncertainties to the GCM simulation and largely limits their applicability (e.g. Chen et al., 2012;Diaz-Nieto and
337 Wilby, 2005). Therefore, although GCM results may be more suitable for large-scale assessments, catchment-
338 scale climate impact assessments are likely to be informed by 'off-line' PET models for the foreseeable future.
339 Consequently, the sensitivity results shown in this study will remain relevant for climate impact assessments
340 conducted using these models.

341 4.2. Relative importance of climate variables affecting PET for different climate zones

342 We now explore the relative importance of each climate variable on overall PET sensitivity, by first visualizing
343 the conditional sensitivity of PET when holding each variable constant at its historical level while perturbing the
344 remaining variables, and then comparing this to the unconditional sensitivity estimates (as shown in Fig. 3 and
345 Fig. 4). Figure 5 shows the ranges of the monthly unconditional PET sensitivity (dashed lines) and the PET
346 sensitivity conditioned on zero-change in each of T , RH , R_s and u_z (solid lines) for the Penman-Monteith model,
347 plotted against the monthly baseline levels of the four climate variables at the 30 study sites.

348 **Figure 5: Monthly PET responses from the Penman-Monteith model, plotted against the monthly baseline levels of (a)**
349 **temperature, (b) relative humidity, (c) solar radiation and (d) wind speed at 30 study sites. Each dashed (solid) line**
350 **represents the range of all PET responses to the full set of climate perturbations (conditioned on no-change in each**
351 **climate variable) for a single month at a single location. The corresponding means are represented by the points on**
352 **the lines. The classification of energy- and water-limited months are based on the corresponding monthly PET/P**
353 **ratios.**

354

355 The figure suggests that perturbations in T have the greatest impact on PET sensitivity compared to other
356 climate variables (Fig. 5a), contributing to at least 45 % of the PET responses compared to the unconditional
357 results. Humidity also plays a significant role, although only for higher humidity levels (contributing up to 57 %
358 of PET responses) with relatively minor influence for the less humid catchments (Fig. 5b). In contrast, the role of
359 solar radiation (Fig. 5c) and wind (Fig. 5d) is generally minor, with the unconditional sensitivities being only
360 slightly wider than the conditional sensitivities.

361 A similar analysis was conducted for the Priestley-Taylor model (Fig. 6), and shows somewhat different results
362 compared to those obtained for the Penman-Monteith model. Consistent with Fig. 5a, temperature has the
363 greatest impact, but in this case contributes up to 85 % of the overall variability (Fig. 6a). As a result, the

364 sensitivity values for the remaining variables are much lower. Unlike in Fig. 5b, the role of relative humidity does
365 not appear to increase significantly with increasing baseline humidity (Fig. 6b) and in general contributes less
366 than 33 % of the overall variability. The lower impact of *RH* on Priestley-Taylor PET compared to the impact on
367 Penman-Monteith PET can be related to the structure of Priestley-Taylor model, which does not consider the
368 aerodynamic processes, so that the impact of *RH* on PET through these processes is not accounted (see Eqn. 2.7,
369 2.15 and 2.16 in Appendix A.2.). The role of solar radiation appears to be somewhat larger for high baseline
370 solar radiation values (Fig. 6c) and wind is shown to have no impact as expected, since wind is not an input into
371 the Priestley-Taylor model (Fig. 6d). However, it is worth noting that although the Priestley-Taylor model does
372 not consider wind as an input variable, the unconditional sensitivity is slightly wider than the sensitivity
373 conditioned on no-change in wind. This is because the conditional sensitivity is estimated with only a subset of
374 all climate perturbations (Sect. 3.4), which may not consist of the entire range of perturbation in each of the
375 other three climate variables.

376 **Figure 6: Monthly PET responses from the Priestley-Taylor model, plotted against the monthly baseline levels of (a)**
377 **temperature, (b) relative humidity, (c) solar radiation and (d) wind speed at 30 study sites. Each dashed (solid) line**
378 **represents the range of all PET responses to the full set of climate perturbations (conditioned on no-change in each**
379 **climate variable) for a single month at a single location. The corresponding means are represented by the points on**
380 **the lines. The classification of energy- and water-limited months are based on the corresponding monthly PET/P**
381 **ratios.**

382

383 A more formal quantitative measure of the relative importance of each climate variable for PET is provided by
384 the Sobol' indices. Figure 7 shows the Sobol' first-order indices of the Penman-Monteith PET to changes in the
385 four climate variables at the annual scale, as well as their interactions. The first-order indices are plotted against
386 the baseline levels of each climatic variable to observe the impact of baseline climate conditions. For
387 presentation purposes, the baseline levels are represented by the rank of the baseline annual average value of

388 each variable, rather than the absolute level of each climate variable across the 30 study sites. The Sobol' indices in the figure show that T is generally the most important variable for PET, with index values ranging from 389 0.46 to 0.62. Since the Sobol' indices suggest the partitioning of the total variance of PET, these results are 390 consistent with Fig. 5a, which suggests that perturbations in T contribute to at least 45 % of the variation in the 391 estimated changes in PET. The role of wind and humidity in affecting the sensitivity values is also evident, with 392 wind being the second-most important variable (with Sobol' indices up to 0.42) for sites with low baseline 393 humidity, and humidity being the second-most important variable (with Sobol' indices up to 0.47) for sites that 394 have high humidity (Fig. 7b). Solar radiation is generally the variable with the lowest Sobol' indices, with the 395 largest contributions (up to 18 %) can be observed for warm catchments (Fig. 7a). 396

397 **Figure 7: Sobol' first-order sensitivity indices of the Penman-Monteith model for changes in the four climate**
398 **variables (colored) and their interaction effects (grey), plotted against the ranking of the average level of each climate**
399 **variable at 30 study sites**
400

401 The Sobol' sensitivity indices are also presented for the Priestley-Taylor model (Fig. 8), and show substantial 402 differences compared to those for the Penman-Monteith model. Temperature exhibits the largest sensitivity 403 score in most cases, and ranges from 0.44 to 0.83. The relative role of temperature varies most clearly as a 404 function of both the baseline temperature (Fig. 8a) and the baseline solar radiation values (Fig. 8c), with 405 temperature being particularly important for low temperature and low solar radiation sites. As temperature and 406 radiation increase, the relative role of solar radiation becomes more important, reaching Sobol' index values of 407 up to 0.49. In contrast, the role of relative humidity is generally minor (with Sobol' indices within the range 408 0.03-0.1) and does not appear to vary as a function of baseline conditions. Finally, the role of wind is absent, 409 given that this variable is not included as part of the Priestley-Taylor equation.

410 **Figure 8: Sobol' first-order sensitivity indices of the Priestley-Taylor model for changes in the four climate variables**
411 **(colored) and their interaction effects (grey), plotted against the ranking of the average level of each climate variable**
412 **at 30 study sites**
413

414 The differences between the Penman-Monteith and Priestley-Taylor models highlight the different physical
415 assumptions underpinning the models, with aerodynamic processes being important for the Penman-Monteith
416 model as indicated by the relative importance of RH and u_z for this model, whereas R_s has a critical role in the
417 Priestley-Taylor model, which is closely linked to the emphasis of radiative energy as the energy source for ET in
418 the model.

419 Finally, comparing Fig. 7 and Fig. 8, it is apparent that the interactions among the four climate variables on PET
420 (shown as grey bars) are greater in the Penman-Monteith model compared to the Priestley-Taylor model.
421 Specifically, these interactions contribute fractions of 0.03-0.04, and 0-0.02 of the total variance in PET for the
422 Penman-Monteith and Priestley-Taylor models, respectively. The relative magnitude of the interaction effects in
423 the two models can be again related to their structural differences: the higher interaction effects in Penman-
424 Monteith can be a result of the larger number of variables in this model compared with those in the Priestley-
425 Taylor model.

426 It is difficult to assess the consistency of these sensitivity results with existing literature, given the different
427 methodologies and datasets used in other studies. Although most PET sensitivity studies used only the Penman-
428 Monteith PET model, there is still substantial discrepancy in results depending on the specific implementations
429 of sensitivity analysis. For example, Gong et al. (2006) perturbed each of temperature, wind speed, relative
430 humidity and solar radiation within $\pm 20\%$ for the Changjiang basin in China, and observed that that relative
431 humidity was generally the most important variable driving PET, followed by solar radiation, temperature and

432 wind speed. This contrasted with our results from the Penman-Monteith model, which showed temperature as
433 the most important variable and solar radiation as the least important variable for almost all the stations
434 analyzed, and may be attributable to the different baseline climates as well as the perturbation ranges used for
435 the sensitivity analysis between the two studies.

436 The results of our study were more consistent with Goyal (2004), who concluded that PET is most sensitive to
437 potential changes in temperature for an arid region in India, by applying a $\pm 20\%$ perturbation on each of
438 temperature, solar radiation, wind speed and vapor pressure. In contrast, Tabari and Hosseinzadeh Talaei
439 (2014) also used a $\pm 20\%$ perturbation range, but on only three climate variables, namely temperature, wind
440 speed and sunshine hours, for several climate regions in Iran. Their study concluded that the catchment aridity
441 was a major determinant of the sensitivity to temperature, wind speed and humidity, whereas our analysis
442 highlights the importance of baseline temperature and humidity, rather than the aridity (or water- or energy-
443 limited status of the catchment) as a key driver.

444 PET sensitivity can further diversify by the choice of PET models, as illustrated in McKenney and Rosenberg
445 (1993), in which the percentage changes in PET due to a $+6\text{ }^\circ\text{C}$ change can differ up to around 40% , when
446 estimated with eight alternative PET models. This lack of consistency in the relative importance of the climate
447 variables for PET is not surprising given the findings of our study, as the results are strongly dependent on the
448 design of the sensitivity analysis experiment, including the choice of study sites and study periods, the input
449 climate variables considered, and the ways to perturb them (i.e. the choice of global or local perturbation and
450 the ranges of perturbation in different input variables).

451 Nevertheless, the sensitivity results from this study suggest some distinct spatial patterns of the relative
452 importance of different climate variables in Australia. Since the Penman-Monteith model is the most

453 comprehensive physically-based PET model, the above regionalization of the PET sensitivity from this model can
454 be used as a benchmark to identify the key climate variables for estimating PET under potential climate change.
455 This information can be particularly useful to suggest the potential suitability of specific PET models for regional
456 applications. For example, since the Penman-Monteith PET showed higher sensitivity to wind at dry locations
457 (Fig. 7b), it is expected that wind-dependent PET models (such as Penman and Penman-Monteith) would be
458 more appropriate for predicting PET at these locations. In contrast, using simpler models that do not consider
459 wind as an input (such as Priestley-Taylor) can be problematic for these locations. Although this study only
460 examined two PET models, the results suggest that simpler empirical models are likely to ignore some potential
461 dynamics and interactions within the climate variables, which makes them less preferred for PET estimation
462 under changing climates.

463 Another particular issue in the selection of one or several PET models under a changing climate arises from
464 considering the current reliability of available climate projections, as the models can show high levels of
465 sensitivity to variables for which we currently do not have high-quality climate projections. For example, for a
466 given emissions scenario, there is reasonable confidence in projections of temperature and relative humidity in
467 Australia, but less confidence in projections of solar radiation and wind (Flato et al., 2013;CSIRO and Bureau of
468 Meteorology, 2015). However the radiation-based Priestley-Taylor model can show high sensitivity to solar
469 radiation, particularly for warm locations with high baseline solar radiation (Fig. 8a and 8c), due to a particular
470 emphasis on radiative energy and thus the empirical relationships between PET and solar radiation. Similarly,
471 the Penman-Monteith model can exhibit higher sensitivity to wind for locations with low relative humidity (Fig.
472 7b). Therefore, the use of GCM projections at these locations may lead to significant uncertainty in PET
473 estimates due to the uncertainty in the driving variables.

474 5. Summary and conclusions

475 In this study, we used a global sensitivity analysis to investigate the sensitivity of PET and the relative
476 importance four climatic variables which influence PET (T , RH , R_s and u_z) under plausible future changes in these
477 variables. The sensitivity analysis was conducted at 30 Australian case study locations within different climate
478 zones to understand the impact of varying baseline hydro-climatic conditions. For the sensitivity analysis, the
479 historical climate data at each study site were first perturbed to represent a large number of plausible climate
480 change conditions, and then the responses in PET were estimated with both the Penman-Monteith and
481 Priestley-Taylor models, from which the sensitivity of PET was analysed. The key results are as follows:

- 482 • In general PET is most sensitive to potential changes in climate in regions with lower temperature, less
483 solar radiation and greater humidity, where two-fold greater changes in PET are expected compared to
484 other locations in Australia.
- 485 • Within the plausible perturbations in T , RH , R_s and u_z , PET is generally most sensitive to T . The relative
486 importance of the other climate variables varies substantially with the PET models. R_s has a dominant
487 role in the radiation-based Priestley-Taylor model, highlighting the importance of radiative energy in
488 the model. In contrast, the importance of RH and u_z are comparable for the Penman-Monteith model,
489 whereas R_s has only little impact, reflecting the contribution of aerodynamic energy.
- 490 • The relative importance of climate variables in influencing PET depends very clearly on baseline climatic
491 conditions. From Penman-Monteith, locations that are warmer, drier and receiving more solar radiation
492 generally show greater sensitivity to u_z and lower sensitivity to RH . For Priestley-Taylor, the importance
493 of T increases while that of R_s decreases for cooler locations and locations receiving less solar radiation.

494 The global sensitivity analysis used in this study is a powerful tool for providing a comprehensive and consistent
495 measure of PET sensitivity to different climatic variables, considering a wide range of possible changes in
496 climate, across different models with different data requirements. However, we have identified space for
497 improvements in further implementations. For example, the bounds of perturbation for each climate variable
498 can have a substantial impact on PET sensitivity, and thus their selection requires careful justification (for
499 example see Whateley et al., 2014;Shin et al., 2013). Therefore, alternative lines of evidence on possible
500 changes in climate should be considered in setting these bounds: for example, the results of ensemble climate
501 models (e.g. Collins et al., 2013), the impact of low-frequency climatic modes (e.g. Chen et al., 2013;Vincent et
502 al., 2015), as well as findings from within paleoclimatology records (e.g. Ault et al., 2014;Ho et al., 2015).

503 The analysis in this study also lends itself to scenario-neutral analyses (Brown et al., 2012;Prudhomme et al.,
504 2010), although the full implications on specific impacts of hydrological systems (e.g. flood risk, water supply,
505 etc) would require the sensitivity analysis to be propagated to runoff via explicitly modelling the interaction
506 between ET and rainfall-runoff processes (e.g. Garcia and Tague, 2015;Roy et al., 2016). Furthermore, potential
507 changes to precipitation, which were not analyzed here but which can have a significant impact on future runoff,
508 would need to be considered. Within this context, the incorporation of alternative lines of evidence can
509 therefore not only be used to define the bounds of the perturbations, but can also be superimposed onto the
510 exposure space (e.g. as in Prudhomme et al., 2013a;Culley et al., 2016) to provide insight into the likelihood of
511 possible changes. The outcomes of our study can feed into such a scenario-neutral analysis by providing
512 guidance on the variables that are likely to be most important for a particular location, as well as providing
513 insights on the potential implications of using alternative PET models on the overall sensitivity results.

514 References

- 515 Akhtar, M., Ahmad, N., and Booij, M. J.: The impact of climate change on the water resources of Hindukush–
516 Karakorum–Himalaya region under different glacier coverage scenarios, *Journal of Hydrology*, 355, 148-163,
517 <http://dx.doi.org/10.1016/j.jhydrol.2008.03.015>, 2008.
- 518 Allen, R. G., Pereira, L. S., Raes, D., and Smith, M.: Crop evapotranspiration–Guidelines for computing crop water
519 requirements–FAO Irrigation and drainage paper 56, FAO, Rome, 300, 6541, 1998.
- 520 Arnell, N. W.: The effect of climate change on hydrological regimes in Europe: a continental perspective, *Global
521 Environmental Change*, 9, 5-23, [http://dx.doi.org/10.1016/S0959-3780\(98\)00015-6](http://dx.doi.org/10.1016/S0959-3780(98)00015-6), 1999.
- 522 Ault, T. R., Cole, J. E., Overpeck, J. T., Pederson, G. T., and Meko, D. M.: Assessing the Risk of Persistent Drought
523 Using Climate Model Simulations and Paleoclimate Data, *Journal of Climate*, 27, 7529-7549, 10.1175/JCLI-D-12-
524 00282.1, 2014.
- 525 Barella-Ortiz, A., Polcher, J., Tuzet, A., and Laval, K.: Potential evaporation estimation through an unstressed
526 surface-energy balance and its sensitivity to climate change, *Hydrol. Earth Syst. Sci.*, 17, 4625-4639,
527 10.5194/hess-17-4625-2013, 2013.
- 528 Bell, V. A., Kay, A. L., Davies, H. N., and Jones, R. G.: An assessment of the possible impacts of climate change on
529 snow and peak river flows across Britain, *Climatic Change*, 136, 539-553, 10.1007/s10584-016-1637-x, 2016.
- 530 Boé, J., and Terray, L.: Uncertainties in summer evapotranspiration changes over Europe and implications for
531 regional climate change, *Geophysical Research Letters*, 35, n/a-n/a, 10.1029/2007GL032417, 2008.
- 532 Brown, C., Ghile, Y., Laverty, M., and Li, K.: Decision scaling: Linking bottom-up vulnerability analysis with
533 climate projections in the water sector, *Water Resources Research*, 48, W09537, 10.1029/2011WR011212, 2012.
- 534 Chang, S., Graham, W. D., Hwang, S., and Muñoz-Carpena, R.: Sensitivity of future continental United States
535 water deficit projections to general circulation models, the evapotranspiration estimation method, and the
536 greenhouse gas emission scenario, *Hydrol. Earth Syst. Sci.*, 20, 3245-3261, 10.5194/hess-20-3245-2016, 2016.
- 537 Chen, H., Xu, C.-Y., and Guo, S.: Comparison and evaluation of multiple GCMs, statistical downscaling and
538 hydrological models in the study of climate change impacts on runoff, *Journal of Hydrology*, 434–435, 36-45,
539 <http://dx.doi.org/10.1016/j.jhydrol.2012.02.040>, 2012.
- 540 Chen, W., Lan, X., Wang, L., and Ma, Y.: The combined effects of the ENSO and the Arctic Oscillation on the
541 winter climate anomalies in East Asia, *Chinese Science Bulletin*, 58, 1355-1362, 10.1007/s11434-012-5654-5,
542 2013.
- 543 Chiew, F. H. S., Teng, J., Vaze, J., Post, D. A., Perraud, J. M., Kirono, D. G. C., and Viney, N. R.: Estimating climate
544 change impact on runoff across southeast Australia: Method, results, and implications of the modeling method,
545 *Water Resources Research*, 45, W10414, 10.1029/2008WR007338, 2009.
- 546 Collins, M., Knutti, R., Arblaster, J., Dufresne, J.-L., Fichet, T., Friedlingstein, P., Gao, X., Gutowski, W. J., Johns,
547 T., Krinner, G., Shongwe, M., Tebaldi, C., Weaver, A. J., and Wehner, M.: Long-term Climate Change: Projections,
548 Commitments and Irreversibility, in: *Climate Change 2013: The Physical Science Basis. Contribution of Working
549 Group I to the Fifth Assessment Report of the Intergovernmental Panel on Climate Change*, edited by: Stocker, T.
550 F., Qin, D., Plattner, G.-K., Tignor, M., Allen, S. K., Boschung, J., Nauels, A., Xia, Y., Bex, V., and Midgley, P. M.,
551 Cambridge University Press, Cambridge, United Kingdom and New York, NY, USA, 1029–1136, 2013.
- 552 CSIRO and Bureau of Meteorology: *Climate Change in Australia Information for Australia’s Natural Resource
553 Management Regions: Technical Report*, CSIRO and Bureau of Meteorology, Australia, 2015.

554 Culley, S., Noble, S., Yates, A., Timbs, M., Westra, S., Maier, H. R., Giuliani, M., and Castelletti, A.: A bottom-up
555 approach to identifying the maximum operational adaptive capacity of water resource systems to a changing
556 climate, *Water Resources Research*, n/a-n/a, 10.1002/2015WR018253, 2016.

557 Diaz-Nieto, J., and Wilby, R. L.: A comparison of statistical downscaling and climate change factor methods:
558 impacts on low flows in the River Thames, United Kingdom, *Climatic Change*, 69, 245-268, 2005.

559 Dingman, S. L.: *Physical Hydrology: Third Edition*, Waveland Press, 2015.

560 Donohue, R. J., McVicar, T. R., and Roderick, M. L.: Generating Australian potential evaporation data suitable for
561 assessing the dynamics in evaporative demand within a changing climate, 2009.

562 Donohue, R. J., McVicar, T. R., and Roderick, M. L.: Can dynamic vegetation information improve the accuracy of
563 Budyko's hydrological model?, *Journal of hydrology*, 390, 23-34, 2010.

564 Ekström, M., Jones, P., Fowler, H., Lenderink, G., Buishand, T., and Conway, D.: Regional climate model data
565 used within the SWURVE project? 1: projected changes in seasonal patterns and estimation of PET, *Hydrology
566 and Earth System Sciences Discussions*, 11, 1069-1083, 2007.

567 Felix, T. P., Petra, D., Stephanie, E., and Martina, F.: Impact of climate change on renewable groundwater
568 resources: assessing the benefits of avoided greenhouse gas emissions using selected CMIP5 climate projections,
569 *Environmental Research Letters*, 8, 024023, 2013.

570 Flato, G., Marotzke, J., Abiodun, B., Braconnot, P., Chou, S. C., Collins, W., Cox, P., Driouech, F., Emori, S., and
571 Eyring, V.: Evaluation of climate models, in: *Climate Change 2013: The Physical Science Basis. Contribution of
572 Working Group I to the Fifth Assessment Report of the Intergovernmental Panel on Climate Change*, Cambridge
573 University Press, 741-866, 2013.

574 Garcia, E. S., and Tague, C. L.: Subsurface storage capacity influences climate–evapotranspiration interactions in
575 three western United States catchments, *Hydrol. Earth Syst. Sci.*, 19, 4845-4858, 10.5194/hess-19-4845-2015,
576 2015.

577 Gerrits, A., Savenije, H., Veling, E., and Pfister, L.: Analytical derivation of the Budyko curve based on rainfall
578 characteristics and a simple evaporation model, *Water Resources Research*, 45, 2009.

579 Gong, L., Xu, C.-y., Chen, D., Halldin, S., and Chen, Y. D.: Sensitivity of the Penman–Monteith reference
580 evapotranspiration to key climatic variables in the Changjiang (Yangtze River) basin, *Journal of Hydrology*, 329,
581 620-629, <http://dx.doi.org/10.1016/j.jhydrol.2006.03.027>, 2006.

582 Gosling, S. N., Taylor, R. G., Arnell, N. W., and Todd, M. C.: A comparative analysis of projected impacts of
583 climate change on river runoff from global and catchment-scale hydrological models, *Hydrol. Earth Syst. Sci.*, 15,
584 279-294, 10.5194/hess-15-279-2011, 2011.

585 Goyal, R. K.: Sensitivity of evapotranspiration to global warming: a case study of arid zone of Rajasthan (India),
586 *Agricultural Water Management*, 69, 1-11, <http://dx.doi.org/10.1016/j.agwat.2004.03.014>, 2004.

587 Guillevic, P., Koster, R. D., Suarez, M. J., Bounoua, L., Collatz, G. J., Los, S. O., and Mahanama, S. P. P.: Influence
588 of the Interannual Variability of Vegetation on the Surface Energy Balance—A Global Sensitivity Study, *Journal
589 of Hydrometeorology*, 3, 617-629, doi:10.1175/1525-7541(2002)003<0617:LOTIVO>2.0.CO;2, 2002.

590 Guo, D., Westra, S., and Maier, H. R.: An inverse approach to perturb historical rainfall data for scenario-neutral
591 climate impact studies, *Journal of Hydrology*, <http://dx.doi.org/10.1016/j.jhydrol.2016.03.025>, 2016a.

592 Guo, D., Westra, S., and Maier, H. R.: An R package for modelling actual, potential and reference
593 evapotranspiration, *Environmental Modelling & Software*, 78, 216-224,
594 <http://dx.doi.org/10.1016/j.envsoft.2015.12.019>, 2016b.

595 Ho, M., Kiem, A. S., and Verdon-Kidd, D. C.: A paleoclimate rainfall reconstruction in the Murray-Darling Basin
596 (MDB), Australia: 1. Evaluation of different paleoclimate archives, rainfall networks, and reconstruction
597 techniques, *Water Resources Research*, 51, 8362-8379, [10.1002/2015WR017058](https://doi.org/10.1002/2015WR017058), 2015.

598 Johnson, F., and Sharma, A.: Measurement of GCM skill in predicting variables relevant for hydroclimatological
599 assessments, *Journal of Climate*, 22, 4373-4382, 2009.

600 Kay, A. L., and Davies, H. N.: Calculating potential evaporation from climate model data: A source of uncertainty
601 for hydrological climate change impacts, *Journal of Hydrology*, 358, 221-239,
602 <http://dx.doi.org/10.1016/j.jhydrol.2008.06.005>, 2008.

603 Kay, A. L., Davies, H. N., Bell, V. A., and Jones, R. G.: Comparison of uncertainty sources for climate change
604 impacts: flood frequency in England, *Climatic Change*, 92, 41-63, [10.1007/s10584-008-9471-4](https://doi.org/10.1007/s10584-008-9471-4), 2009.

605 Kay, A. L., Crooks, S. M., and Reynard, N. S.: Using response surfaces to estimate impacts of climate change on
606 flood peaks: assessment of uncertainty, *Hydrological Processes*, 28, 5273-5287, [10.1002/hyp.10000](https://doi.org/10.1002/hyp.10000), 2014.

607 Koedyk, L. P., and Kingston, D. G.: Potential evapotranspiration method influence on climate change impacts on
608 river flow: a mid-latitude case study, *Hydrology Research*, [10.2166/nh.2016.152](https://doi.org/10.2166/nh.2016.152), 2016.

609 Köppen, W., Geiger, R., Borchardt, W., Wegener, K., Wagner, A., Knoch, K., Sapper, K., Ward, R. D., Brooks, C. F.,
610 and Connor, A.: *Handbuch der klimatologie*, 1, Gebrüder Borntraeger Berlin, Germany, 1930.

611 Köppen, W. P.: *Grundriss der klimakunde*, 1931.

612 Li, L., Maier, H. R., Partington, D., Lambert, M. F., and Simmons, C. T.: Performance assessment and
613 improvement of recursive digital baseflow filters for catchments with different physical characteristics and
614 hydrological inputs, *Environmental Modelling & Software*, 54, 39-52,
615 <http://dx.doi.org/10.1016/j.envsoft.2013.12.011>, 2014.

616 Lu, X., Bai, H., and Mu, X.: Explaining the evaporation paradox in Jiangxi Province of China: Spatial distribution
617 and temporal trends in potential evapotranspiration of Jiangxi Province from 1961 to 2013, *International Soil
618 and Water Conservation Research*, 4, 45-51, <http://dx.doi.org/10.1016/j.iswcr.2016.02.004>, 2016.

619 McKenney, M. S., and Rosenberg, N. J.: Sensitivity of some potential evapotranspiration estimation methods to
620 climate change, *Agricultural and Forest Meteorology*, 64, 81-110, [http://dx.doi.org/10.1016/0168-
621 1923\(93\)90095-Y](http://dx.doi.org/10.1016/0168-1923(93)90095-Y), 1993.

622 McMahan, T. A., Peel, M. C., Lowe, L., Srikanthan, R., and McVicar, T. R.: Estimating actual, potential, reference
623 crop and pan evaporation using standard meteorological data: a pragmatic synthesis, *Hydrol. Earth Syst. Sci.*, 17,
624 1331-1363, [10.5194/hess-17-1331-2013](https://doi.org/10.5194/hess-17-1331-2013), 2013.

625 McVicar, T. R., Van Niel, T. G., Li, L. T., Roderick, M. L., Rayner, D. P., Ricciardulli, L., and Donohue, R. J.: Wind
626 speed climatology and trends for Australia, 1975 – 2006: Capturing the stilling phenomenon and comparison
627 with near - surface reanalysis output, *Geophysical Research Letters*, 35, 2008.

628 McVicar, T. R., Donohue, R. J., O'Grady, A. P., and Li, L.: The effects of climatic changes on plant physiological
629 and catchment ecohydrological processes in the high-rainfall catchments of the Murray-Darling Basin: A scoping
630 study, Prepared for the Murray-Darling Basin Authority (MDBA) by the Commonwealth Scientific and Industrial
631 Research Organization (CSIRO) Water for a Healthy Country National Research Flagship, MDBA, Canberra, ACT,
632 Australia, 2010.

633 McVicar, T. R., Roderick, M. L., Donohue, R. J., Li, L. T., Van Niel, T. G., Thomas, A., Grieser, J., Jhajharia, D., Himri,
634 Y., Mahowald, N. M., Mescherskaya, A. V., Kruger, A. C., Rehman, S., and Dinpashoh, Y.: Global review and
635 synthesis of trends in observed terrestrial near-surface wind speeds: Implications for evaporation, *Journal of
636 Hydrology*, 416–417, 182-205, <http://dx.doi.org/10.1016/j.jhydrol.2011.10.024>, 2012.

637 Milly, P. C. D., and Dunne, K. A.: Potential evapotranspiration and continental drying, *Nature Clim. Change*,
638 advance online publication, 10.1038/nclimate3046

639 <http://www.nature.com/nclimate/journal/vaop/ncurrent/abs/nclimate3046.html#supplementary-information>,
640 2016.

641 Nossent, J., Elsen, P., and Bauwens, W.: Sobol' sensitivity analysis of a complex environmental model,
642 *Environmental Modelling & Software*, 26, 1515-1525, 2011.

643 Osidle, O., and Beck, M.: Identification of model structure for aquatic ecosystems using regionalized sensitivity
644 analysis, *Water Science & Technology*, 43, 271-278, 2001.

645 Oudin, L., Hervieu, F., Michel, C., Perrin, C., Andréassian, V., Anctil, F., and Loumagne, C.: Which potential
646 evapotranspiration input for a lumped rainfall-runoff model?: Part 2—Towards a simple and efficient potential
647 evapotranspiration model for rainfall-runoff modelling, *Journal of Hydrology*, 303, 290-306,
648 <http://dx.doi.org/10.1016/j.jhydrol.2004.08.026>, 2005.

649 Paton, F. L., Maier, H. R., and Dandy, G. C.: Relative magnitudes of sources of uncertainty in assessing climate
650 change impacts on water supply security for the southern Adelaide water supply system, *Water Resources*
651 *Research*, 49, 1643-1667, 10.1002/wrcr.20153, 2013.

652 Paton, F. L., Maier, H. R., and Dandy, G. C.: Including adaptation and mitigation responses to climate change in a
653 multiobjective evolutionary algorithm framework for urban water supply systems incorporating GHG emissions,
654 *Water Resources Research*, 50, 6285-6304, 10.1002/2013WR015195, 2014.

655 Prudhomme, C., Wilby, R. L., Crooks, S., Kay, A. L., and Reynard, N. S.: Scenario-neutral approach to climate
656 change impact studies: Application to flood risk, *Journal of Hydrology*, 390, 198-209,
657 <http://dx.doi.org/10.1016/j.jhydrol.2010.06.043>, 2010.

658 Prudhomme, C., Crooks, S., Kay, A., and Reynard, N.: Climate change and river flooding: part 1 classifying the
659 sensitivity of British catchments, *Climatic Change*, 119, 933-948, 10.1007/s10584-013-0748-x, 2013a.

660 Prudhomme, C., Kay, A. L., Crooks, S., and Reynard, N.: Climate change and river flooding: Part 2 sensitivity
661 characterisation for british catchments and example vulnerability assessments, *Climatic Change*, 119, 949-964,
662 10.1007/s10584-013-0726-3, 2013b.

663 Prudhomme, C., and Williamson, J.: Derivation of RCM-driven potential evapotranspiration for hydrological
664 climate change impact analysis in Great Britain: a comparison of methods and associated uncertainty in future
665 projections, *Hydrology and Earth System Sciences*, 17, 1365-1377, 2013.

666 Ravazzani, G., Ghilardi, M., Mendlik, T., Gobiet, A., Corbari, C., and Mancini, M.: Investigation of Climate Change
667 Impact on Water Resources for an Alpine Basin in Northern Italy: Implications for Evapotranspiration Modeling
668 Complexity, *PLOS ONE*, 9, e109053, 10.1371/journal.pone.0109053, 2014.

669 Roderick, M. L., and Farquhar, G. D.: The Cause of Decreased Pan Evaporation over the Past 50 Years, *Science*,
670 298, 1410-1411, 10.1126/science.1075390-a, 2002.

671 Roderick, M. L., Rotstayn, L. D., Farquhar, G. D., and Hobbins, M. T.: On the attribution of changing pan
672 evaporation, *Geophysical research letters*, 34, 2007.

673 Roy, T., Gupta, H. V., Serrat-Capdevila, A., and Valdes, J. B.: Using Satellite-Based Evapotranspiration Estimates
674 to Improve the Structure of a Simple Conceptual Rainfall-Runoff Model, *Hydrol. Earth Syst. Sci. Discuss.*, 2016, 1-
675 28, 10.5194/hess-2016-413, 2016.

676 Rustomji, P., Bennett, N., and Chiew, F.: Flood variability east of Australia's great dividing range, *Journal of*
677 *Hydrology*, 374, 196-208, 2009.

678 Saltelli, A., Annoni, P., Azzini, I., Campolongo, F., Ratto, M., and Tarantola, S.: Variance based sensitivity analysis
679 of model output. Design and estimator for the total sensitivity index, *Computer Physics Communications*, 181,
680 259-270, <http://dx.doi.org/10.1016/j.cpc.2009.09.018>, 2010.

681 Seneviratne, S. I., Wilhelm, M., Stanelle, T., van den Hurk, B., Hagemann, S., Berg, A., Cheruy, F., Higgins, M. E.,
682 Meier, A., Brovkin, V., Claussen, M., Ducharne, A., Dufresne, J.-L., Findell, K. L., Ghattas, J., Lawrence, D. M.,
683 Malyshev, S., Rummukainen, M., and Smith, B.: Impact of soil moisture-climate feedbacks on CMIP5 projections:
684 First results from the GLACE-CMIP5 experiment, *Geophysical Research Letters*, 40, 5212-5217,
685 10.1002/grl.50956, 2013.

686 Shin, M.-J., Guillaume, J. H. A., Croke, B. F. W., and Jakeman, A. J.: Addressing ten questions about conceptual
687 rainfall-runoff models with global sensitivity analyses in R, *Journal of Hydrology*, 503, 135-152,
688 <http://dx.doi.org/10.1016/j.jhydrol.2013.08.047>, 2013.

689 Sieber, A., and Uhlenbrook, S.: Sensitivity analyses of a distributed catchment model to verify the model
690 structure, *Journal of Hydrology*, 310, 216-235, <http://dx.doi.org/10.1016/j.jhydrol.2005.01.004>, 2005.

691 Sobol', I. M., Tarantola, S., Gatelli, D., Kucherenko, S. S., and Mauntz, W.: Estimating the approximation error
692 when fixing unessential factors in global sensitivity analysis, *Reliability Engineering & System Safety*, 92, 957-960,
693 <http://dx.doi.org/10.1016/j.ress.2006.07.001>, 2007.

694 Steinschneider, S., and Brown, C.: A semiparametric multivariate, multi-site weather generator with low-
695 frequency variability for use in climate risk assessments, *Water Resources Research*, n/a-n/a,
696 10.1002/wrcr.20528, 2013.

697 Stern, H., De Hoedt, G., and Ernst, J.: Objective classification of Australian climates, *Australian Meteorological*
698 *Magazine*, 49, 87-96, 2000.

699 Stocker, T. F., Qin, D., Plattner, G.-K., Tignor, M., Allen, S. K., Boschung, J., Nauels, A., Xia, Y., Bex, V., and
700 Midgley, P. M.: Climate change 2013: The physical science basis, Intergovernmental Panel on Climate Change,
701 Working Group I Contribution to the IPCC Fifth Assessment Report (AR5)(Cambridge Univ Press, New York),
702 2013.

703 Tabari, H., and Hosseinzadeh Talaee, P.: Sensitivity of evapotranspiration to climatic change in different climates,
704 *Global and Planetary Change*, 115, 16-23, <http://dx.doi.org/10.1016/j.gloplacha.2014.01.006>, 2014.

705 Tang, Y., Reed, P., van Werkhoven, K., and Wagener, T.: Advancing the identification and evaluation of
706 distributed rainfall-runoff models using global sensitivity analysis, *Water Resources Research*, 43, n/a-n/a,
707 10.1029/2006WR005813, 2007a.

708 Tang, Y., Reed, P., Wagener, T., and Van Werkhoven, K.: Comparing sensitivity analysis methods to advance
709 lumped watershed model identification and evaluation, *Hydrology and Earth System Sciences Discussions*, 11,
710 793-817, 2007b.

711 Tang, Y., Reed, P., Wagener, T., and van Werkhoven, K.: Comparing sensitivity analysis methods to advance
712 lumped watershed model identification and evaluation, *Hydrol. Earth Syst. Sci.*, 11, 793-817, 10.5194/hess-11-
713 793-2007, 2007c.

714 Taylor, I. H., Burke, E., McColl, L., Falloon, P. D., Harris, G. R., and McNeall, D.: The impact of climate mitigation
715 on projections of future drought, *Hydrol. Earth Syst. Sci.*, 17, 2339-2358, 10.5194/hess-17-2339-2013, 2013.

716 van Griensven, A., Meixner, T., Grunwald, S., Bishop, T., Diluzio, M., and Srinivasan, R.: A global sensitivity
717 analysis tool for the parameters of multi-variable catchment models, *Journal of Hydrology*, 324, 10-23,
718 <http://dx.doi.org/10.1016/j.jhydrol.2005.09.008>, 2006.

719 Vincent, L. A., Zhang, X., Brown, R. D., Feng, Y., Mekis, E., Milewska, E. J., Wan, H., and Wang, X. L.: Observed
720 Trends in Canada's Climate and Influence of Low-Frequency Variability Modes, *Journal of Climate*, 28, 4545-
721 4560, 10.1175/JCLI-D-14-00697.1, 2015.

722 Whateley, S., Steinschneider, S., and Brown, C.: A climate change range - based method for estimating
723 robustness for water resources supply, *Water Resources Research*, 50, 8944-8961, 2014.

724 Wilby, R. L., Whitehead, P. G., Wade, A. J., Butterfield, D., Davis, R. J., and Watts, G.: Integrated modelling of
725 climate change impacts on water resources and quality in a lowland catchment: River Kennet, UK, *Journal of*
726 *Hydrology*, 330, 204-220, <http://dx.doi.org/10.1016/j.jhydrol.2006.04.033>, 2006.

727 Zhang, X. Y., Trame, M. N., Lesko, L. J., and Schmidt, S.: Sobol Sensitivity Analysis: A Tool to Guide the
728 Development and Evaluation of Systems Pharmacology Models, *CPT: Pharmacometrics & Systems*
729 *Pharmacology*, 4, 69-79, 10.1002/psp4.6, 2015.

730

731

732 Appendix

733 A.1. Sobol' sensitivity analysis (Sobol' et al., 2007)

734 Sobol' is considered a variance-based method, which requires estimation of the total variance in a model output
735 due to changes in its inputs is estimated with a Monte-Carlo approach. To estimate the variances, a large
736 number of samples is firstly drawn by varying all input variables simultaneously, and then a Sobol' sequence is
737 constructed by re-sampling from within these Monte-Carlo samples (Saltelli et al., 2010). According to Sobol' et
738 al. (2007), to estimate the Sobol' first-order and total-order indices with a Monte-Carlo sample size of n
739 consisting of p input variables, a Sobol' sequence with a total of $n.(p+2)$ samples should be obtained, i.e.
740 requiring $n.(p+2)$ model evaluations.

741 Sobol' analysis partitions the total variance in model output to the contribution of each individual input variable
742 (i.e. first-order effects), as well as their interactions (i.e. higher-order effects), as follows (equation adapted
743 from Zhang et al., 2015):

$$744 \quad V_Y = \sum_{i=1}^n V_i \quad + \quad \sum_{i<j} V_{ij} + \sum_{i<j<k} V_{ijk} \dots + V_{1,2,\dots,n} \quad (1.1)$$

745 **Individual effects** **Interactions**

746 The outputs from Sobol' analysis include (equations adapted from Nossent et al., 2011):

- 747 1) First-order sensitivity index, which quantifies the individual contribution of each input variable to
748 the total variance of the model's output;

$$749 \quad S_i = \frac{V_i}{V_Y} \quad (1.2)$$

2) Second- and higher-order sensitivity index, which quantifies the contribution of interactions among two or more input variables to the total variance of the model's output;

$$\text{For second-order: } S_{ij} = \frac{V_{ij}}{V_Y} \quad (1.3)$$

$$\text{For higher-order: } S_{ij\dots n} = \frac{V_{ij\dots n}}{V_Y} \quad (1.4)$$

3) Total sensitivity index, which quantifies the total contribution of each input variable, including its individual effect as well as all its interactions with other input variables, to the total variance of the model's output.

$$S_{Ti} = S_i + \sum_{j \neq i} S_{ij} = 1 - \frac{V_{\sim i}}{V_Y} \quad (1.5)$$

From Eqn. 1.1 to 1.4, the sum of individual effects of all input variables and all their interactions equals one (adapted from Zhang et al., 2015):

$$1 = \sum_{i=1}^n S_i + \sum_{i < j} S_{ij} + \sum_{i < j < k} S_{ijk} \dots + S_{1,2,\dots,n} \quad (1.6)$$

Individual effects

Interactions

763 A.2. Penman-Monteith PET model (FAO-56) (as in McMahon et al., 2013)

764 The Penman-Monteith PET model (FAO-56) is given as:

765
$$ET = \frac{0.408\Delta(R_n - G) + \gamma \frac{900}{T_a + 273} u_2 (v_a^* - v_a)}{\Delta + \gamma(1 + 0.34u_2)} \quad (2.1)$$

766
767 The process for estimating each of the variables in this equation are described in the following sections.
768

769 *Estimating Δ in Equation 2.1*

770 Δ is the slope of vapor pressure curve in $\text{kPa}^\circ\text{C}^{-1}$, which is estimated by:

771
$$\Delta = \frac{4098[0.6108 \exp(\frac{17.27 + T_a}{T_a + 237.3})]}{(T_a + 237.3)^2} \quad (2.2)$$

772
773 In Eqn. 2.2, T_a is the average daily temperature in $^\circ\text{C}$, calculated as:

774
$$T_a = \frac{T_{max} + T_{min}}{2} \quad (2.3)$$

775

776 *Estimating R_n in Equation 2.1*

777 R_n is the net incoming solar radiation at the evaporative surface in $\text{MJ.m}^{-2}.\text{day}^{-1}$, which is estimated by:

778
$$R_n = R_{ns} - R_{nl} \quad (2.4)$$

779

780 In Eqn. 2.4, R_{ns} is the net shortwave solar radiation, estimated by:

781
$$R_{ns} = (1 - \alpha)R_s \quad (2.5)$$

782

783 In Eqn. 2.5, α is the albedo at evaporative surface which is fixed at 0.23 in this equation, and R_s is the measured
784 or estimated incoming solar radiation in $\text{MJ.m}^{-2}.\text{day}^{-1}$. R_{nl} is the net outgoing longwave radiation, estimated as:

785

786
$$R_{nl} = \sigma(0.34 - 0.14v_a^{0.5}) \frac{(T_{max} + 237.2)^4 + (T_{min} + 237.2)^4}{2} (1.35 \frac{R_s}{R_{s0}} - 0.35) \quad (2.6)$$

787

788 In Eqn. 2.6: σ is Stefan-Boltzmann constant = $4.903 \times 10^{-9} \text{ MJ.m}^{-2}.\text{day}^{-1} \text{ }^\circ\text{K}^{-4}$, v_a is the mean daily actual vapor
789 pressure in kPa , R_{s0} is the clear-sky radiation in $\text{MJ.m}^{-2}.\text{day}^{-1}$. v_a and R_{s0} estimated by Eqn. 2.7 and 2.8,
790 respectively:

791
$$v_a = \frac{v_a^*(T_{max}) \frac{RH_{max}}{100} + v_a^*(T_{min}) \frac{RH_{min}}{100}}{2} \quad (2.7)$$

792

793
$$R_{s0} = (0.75 + 2 \times 10^{-5} Elev) R_a \quad (2.8)$$

794

795 In Eqn. 2.8, $Elev$ is the ground elevation above sea level at the measurement location, and R_a is the
 796 extraterrestrial solar radiation in $\text{MJ.m}^{-2}.\text{day}^{-1}$, estimated as:

$$797 \quad R_a = \frac{1440}{\pi} G_{sc} d_r^2 (\omega_s \sin(lat) \sin(\delta) + \cos(lat) \sin(lat) \sin(\omega_s)) \quad (2.9)$$

798
 799 In Eqn. 2.9, G_{sc} is the solar constant = $0.0820 \text{ MJ.m}^{-2}.\text{min}^{-1}$, lat is the latitude in radian, d_r is the inverse relative
 800 distance between Earth and Sun, δ is the solar declination in radians, and ω_s is the sunset hour angle in radians,
 801 The d_r , δ and ω_s are estimated as follows:

$$802 \quad d_r^2 = 1 + 0.033 \cos\left(\frac{2\pi}{365} DoY\right) \text{ with } DoY \text{ as the day of the year} \quad (2.10)$$

$$803 \quad \delta = 0.409 \sin\left(\frac{2\pi}{365} DoY - 1.39\right) \quad (2.11)$$

$$804 \quad \omega_s = \arccos[-\tan(lat) \tan(\delta)] \quad (2.12)$$

805

806 *Estimating other variables in Equation 2.1*

807 - G is negligible for daily time step.

808
 809 - γ is the psychrometric constant in $\text{kPa}^\circ\text{C}^{-1}$, estimated as:

$$810 \quad \gamma = 0.00163 \frac{P}{\lambda} \text{ where } P \text{ is the pressure at elevation } z \text{ meters} \quad (2.13)$$

811
 812 - u_2 is the daily average wind speed measured at 2 meters in m.s^{-1} , which can be estimated from the
 813 measured wind speed at z meters as:

$$814 \quad u_2 = u_z \frac{\ln\left(\frac{2}{z_0}\right)}{\ln\left(\frac{z}{z_0}\right)} \text{ where } z_0 \text{ is the roughness height in meters} \quad (2.14)$$

815
 816 - $(v_a^* - v_a)$ is the vapour pressure deficit in kPa, in which v_a is the mean daily actual vapor pressure in kPa,
 817 estimated as Eqn. 2.7; v_a^* is the daily saturation vapor pressure in kPa, estimated as:

$$818 \quad v_a^* = \frac{v_a^*(T_{max}) + v_a^*(T_{min})}{2} \quad (2.15)$$

819
 820 In Eqn. 2.15, $v_a^*(T_{max})$ and $v_a^*(T_{min})$ are the vapor pressures at temperatures T_{max} and T_{min} in $^\circ\text{C}$ are estimated
 821 with:

$$822 \quad v_T^* = 0.6108 \exp\left[\frac{17.27T}{T+237.3}\right] \quad (2.16)$$

823

824

825 A.3. Priestley-Taylor PET model (as in McMahon et al., 2013)

826 The Priestley-Taylor PET model is given as:

827

$$ET = \alpha_{PT} * \left[\frac{\Delta}{\Delta + \gamma} \frac{R_n}{\lambda} - \frac{G}{\lambda} \right] \quad (3.1)$$

828 where:

829

830

831

832

833

834

835

836

837

838

839

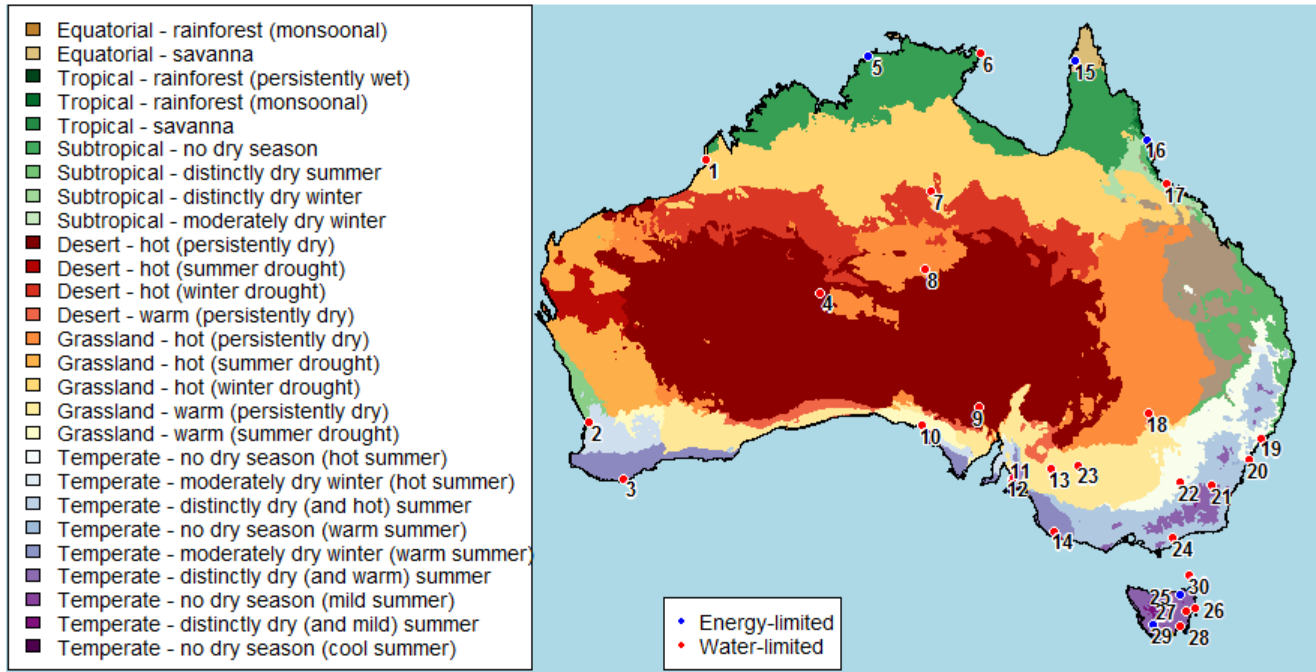
840

841

842

843

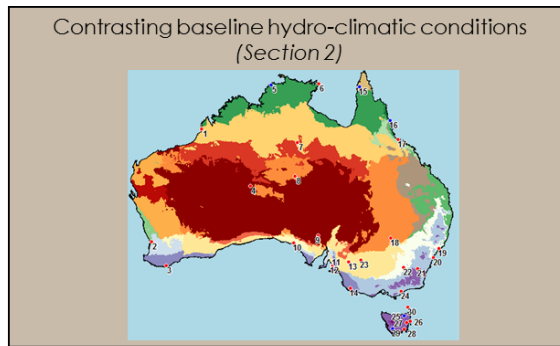
- α_{PT} is the albedo specifically used for the Priestley-Taylor model, since an evaporative surface of reference crop was assumed, this has a value of 1.12 which was for a similar surface of short grass (See Table S8 of the supplementary of McMahon et al., 2013),
- Δ is the slope of vapor pressure curve in $\text{kPa}^\circ\text{C}^{-1}$, estimated as Eqn 2.2.
- γ is the psychrometric constant in $\text{kPa}^\circ\text{C}^{-1}$, estimated as Eqn. 2.12.
- λ is the latent heat of vaporization, which is 2.45 MJ.kg^{-1} at 20°C .
- R_n is the net incoming solar radiation at the evaporative surface in $\text{MJ.m}^{-2}\text{day}^{-1}$, which is estimated in the same way as Eqn. 2.4.
- G is negligible for daily time step.



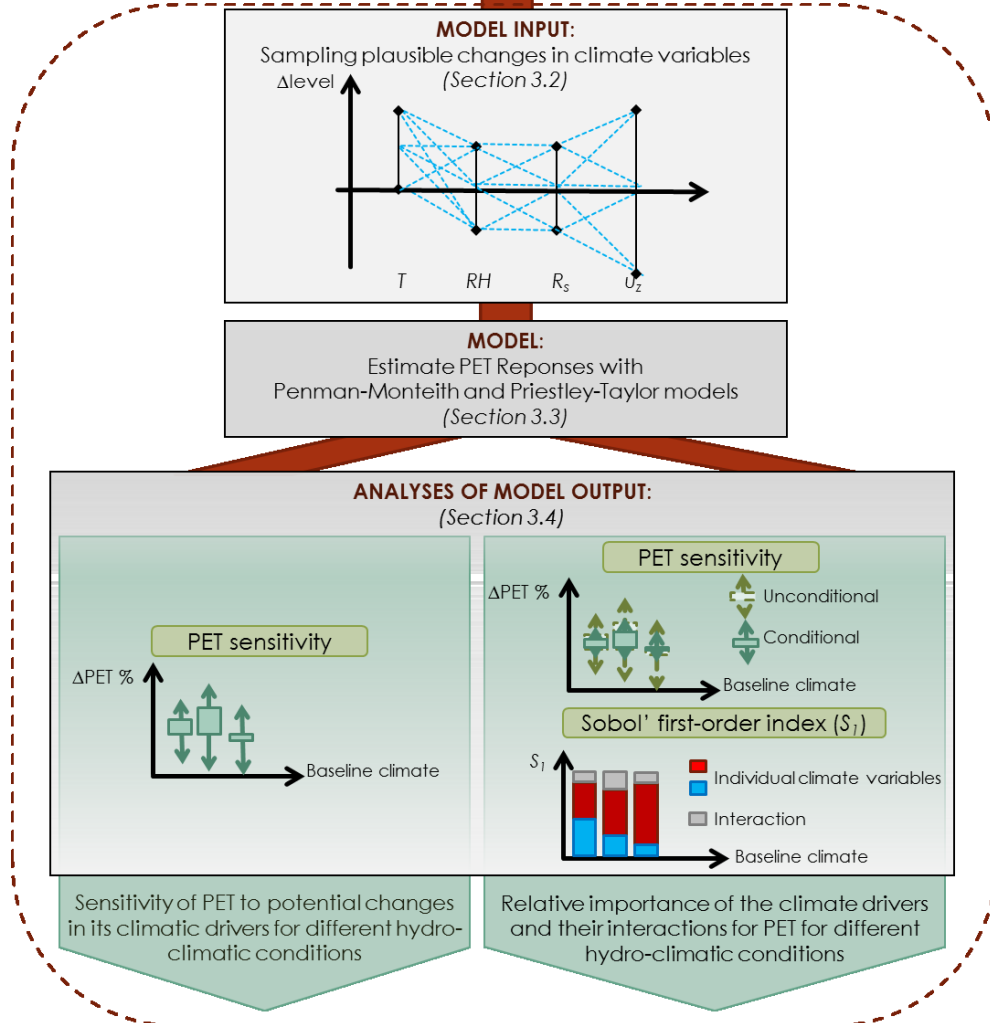
845

846 **Figure 1: Locations of 30 Australian weather stations (see Table 1 for the full names of these weather stations)**
 847 **selected for analysis, with reference to their corresponding climate classes derived following the modified Köppen**
 848 **classification (reproduced with data from Stern et al., 2000).**

849



Global Sensitivity Analysis

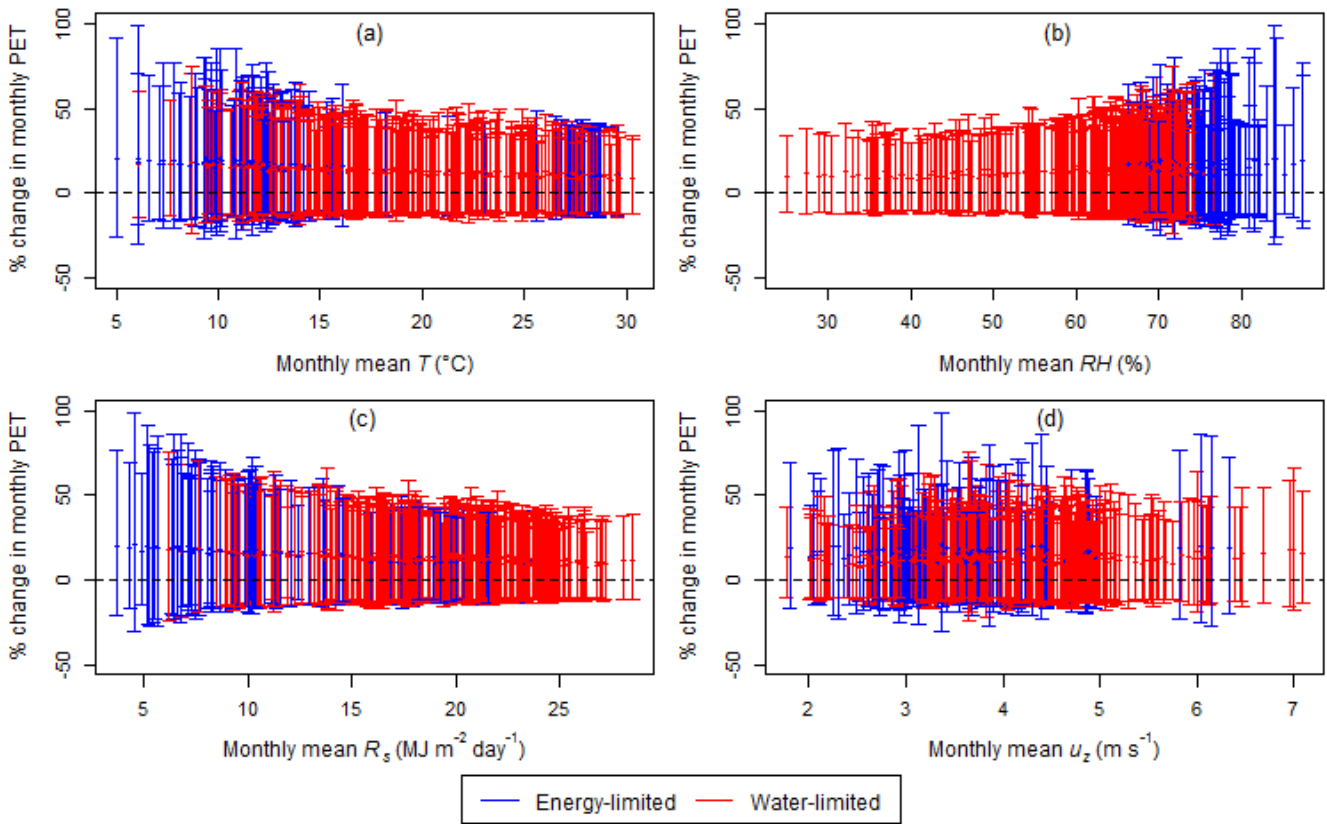


850

851

852

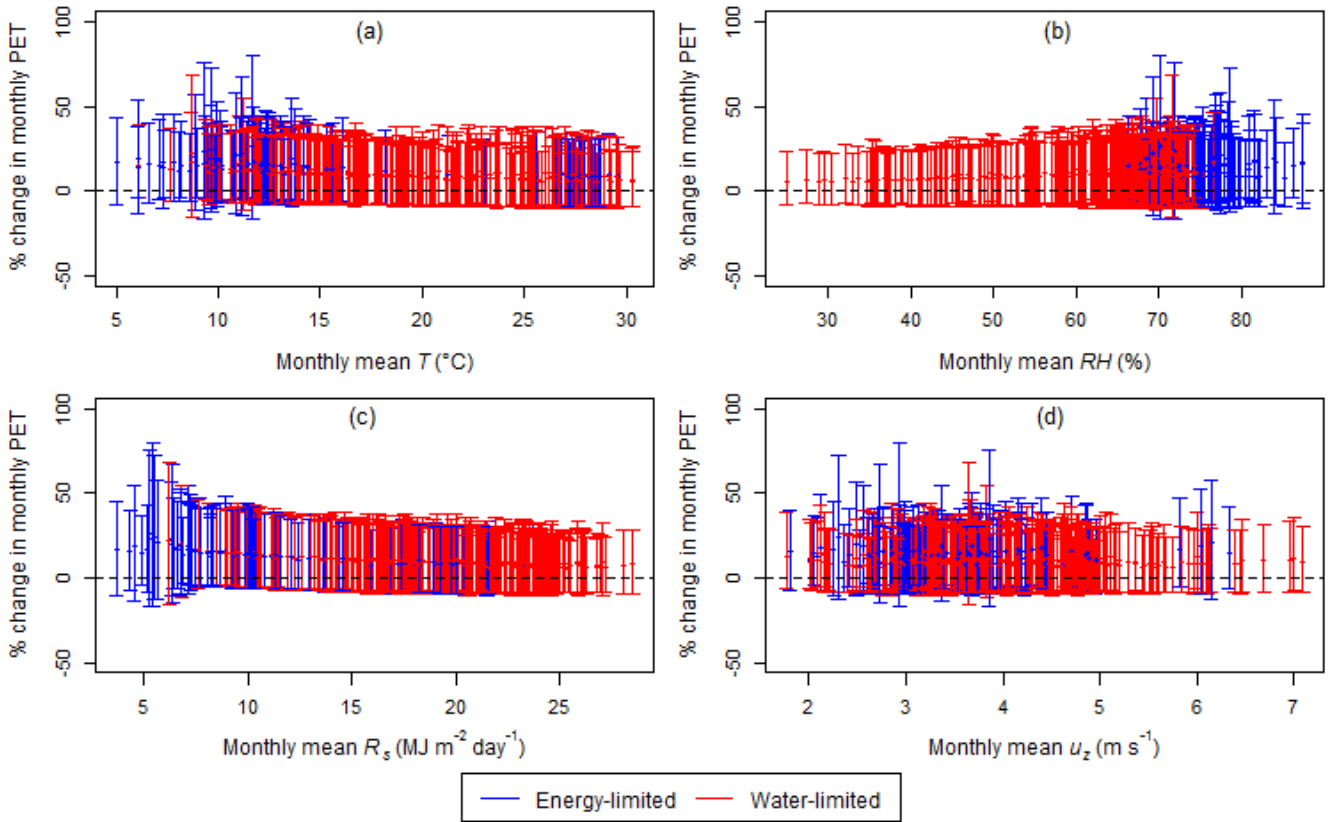
Figure 2: Schematic of the method used in this study.



853

854 **Figure 3: Monthly PET responses from the Penman-Monteith model, plotted against the monthly baseline levels of (a)**
 855 **temperature, (b) relative humidity, (c) solar radiation and (d) wind speed at 30 study sites. Each interval represents**
 856 **the range of all PET responses to the full set of climate perturbations for a single month at a single location, with the**
 857 **mean represented by the point on the line. The classification of energy- and water-limited months are based on the**
 858 **corresponding monthly PET/P ratios.**

859

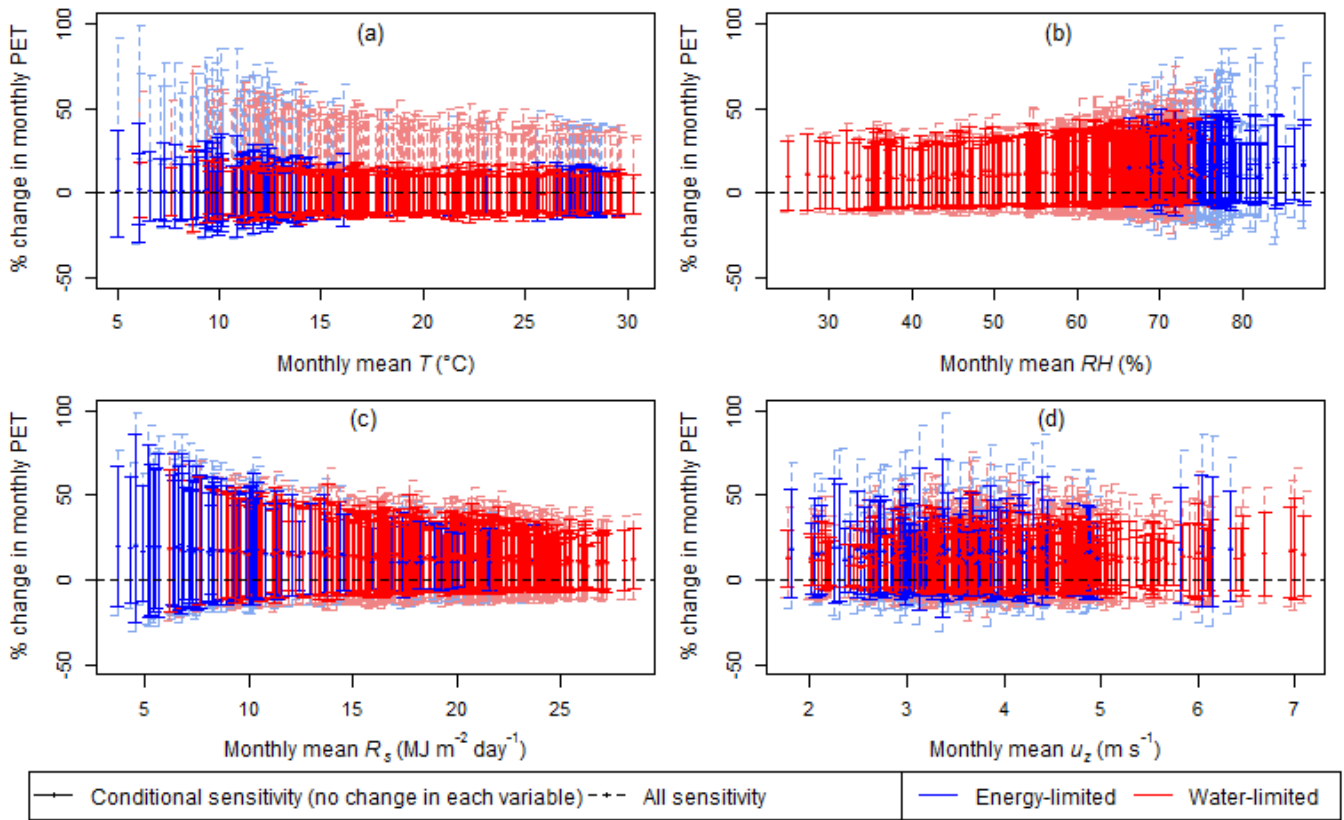


860

861 **Figure 4: Monthly PET responses from the Priestley-Taylor model, plotted against the monthly baseline levels of (a)**
 862 **temperature, (b) relative humidity, (c) solar radiation and (d) wind speed at 30 study sites. Each interval represents**
 863 **the range of all PET responses to the full set of climate perturbations for a single month at a single location, with the**
 864 **mean represented by the point on the line. The classification of energy- and water-limited months are based on the**
 865 **corresponding monthly PET/P ratios.**

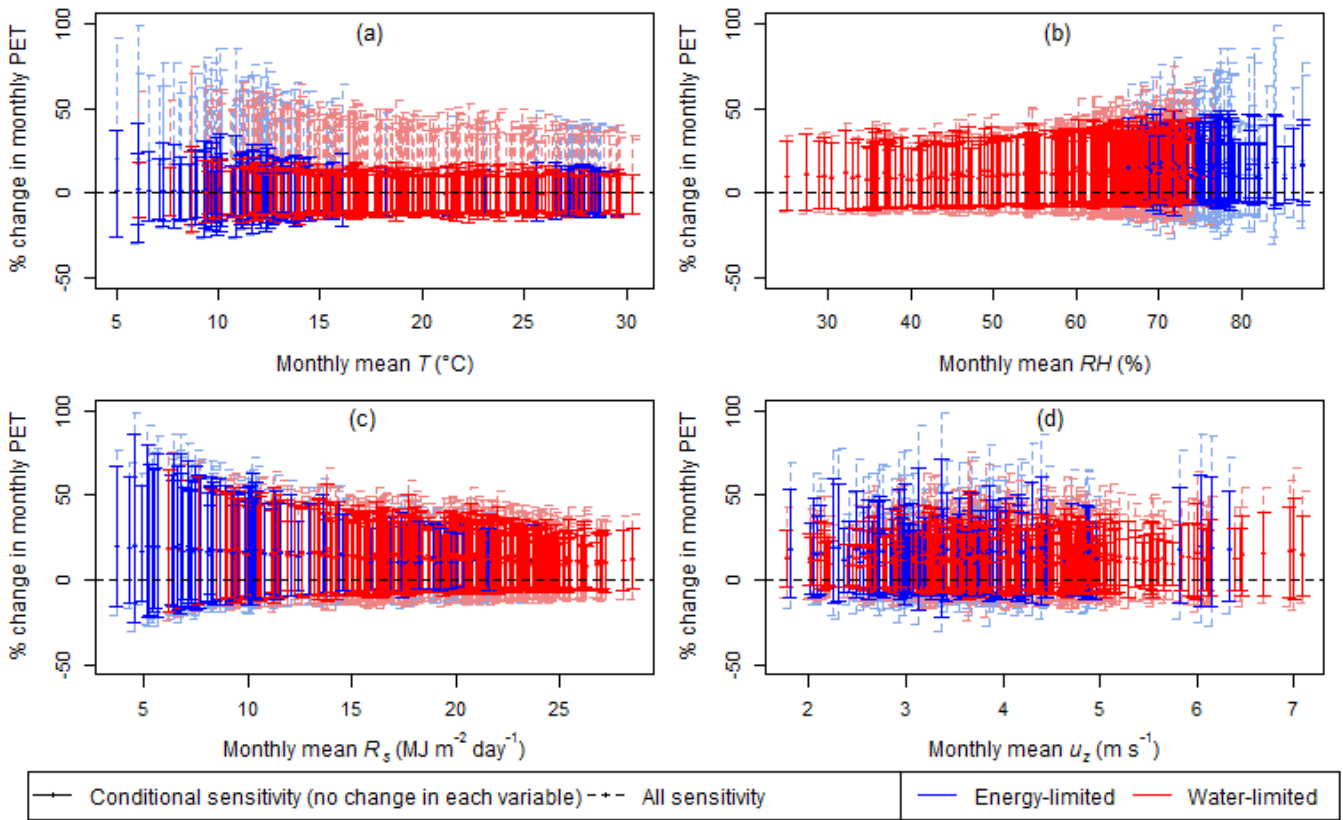
866

867



868

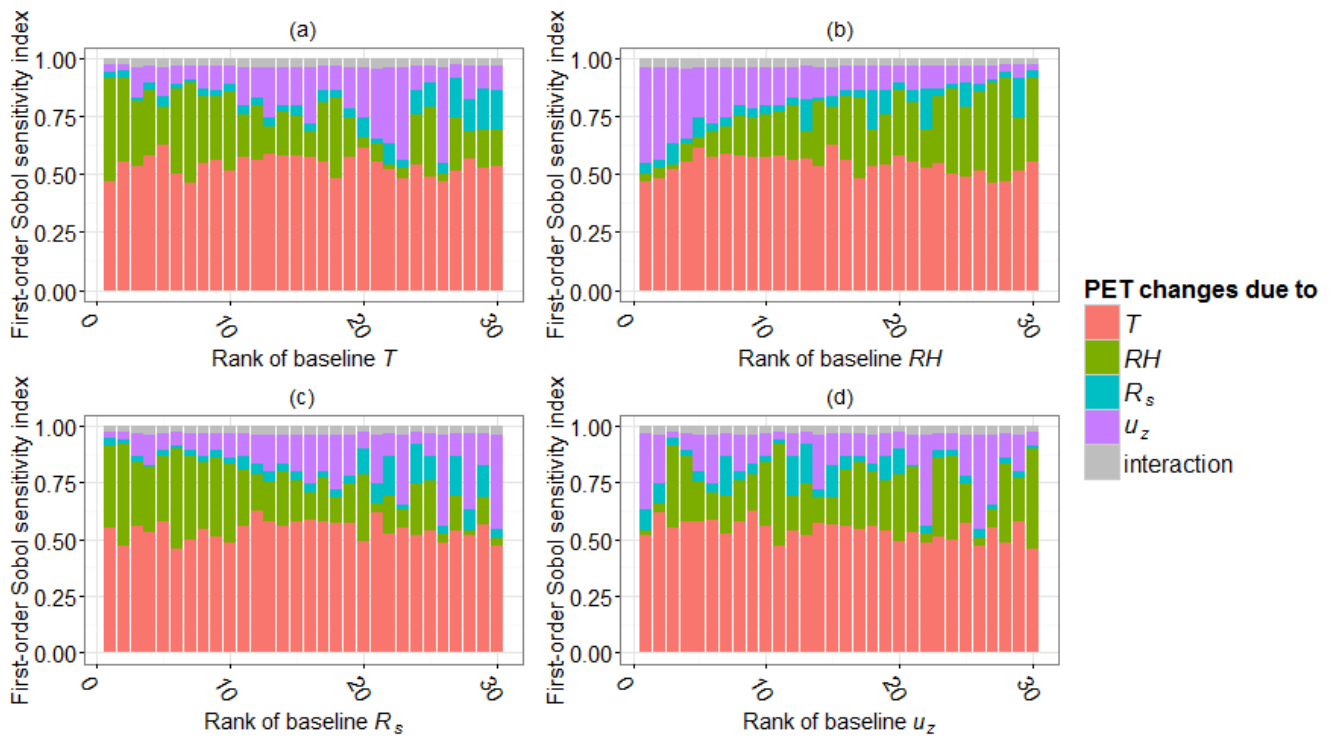
869 **Figure 5: Monthly PET responses from the Penman-Monteith model, plotted against the monthly baseline levels of (a)**
 870 **temperature, (b) relative humidity, (c) solar radiation and (d) wind speed at 30 study sites. Each dashed (solid) line**
 871 **represents the range of all PET responses to the full set of climate perturbations (conditioned on no-change in each**
 872 **climate variable) for a single month at a single location. The corresponding means are represented by the points on**
 873 **the lines. The classification of energy- and water-limited months are based on the corresponding monthly PET/P**
 874 **ratios.**
 875



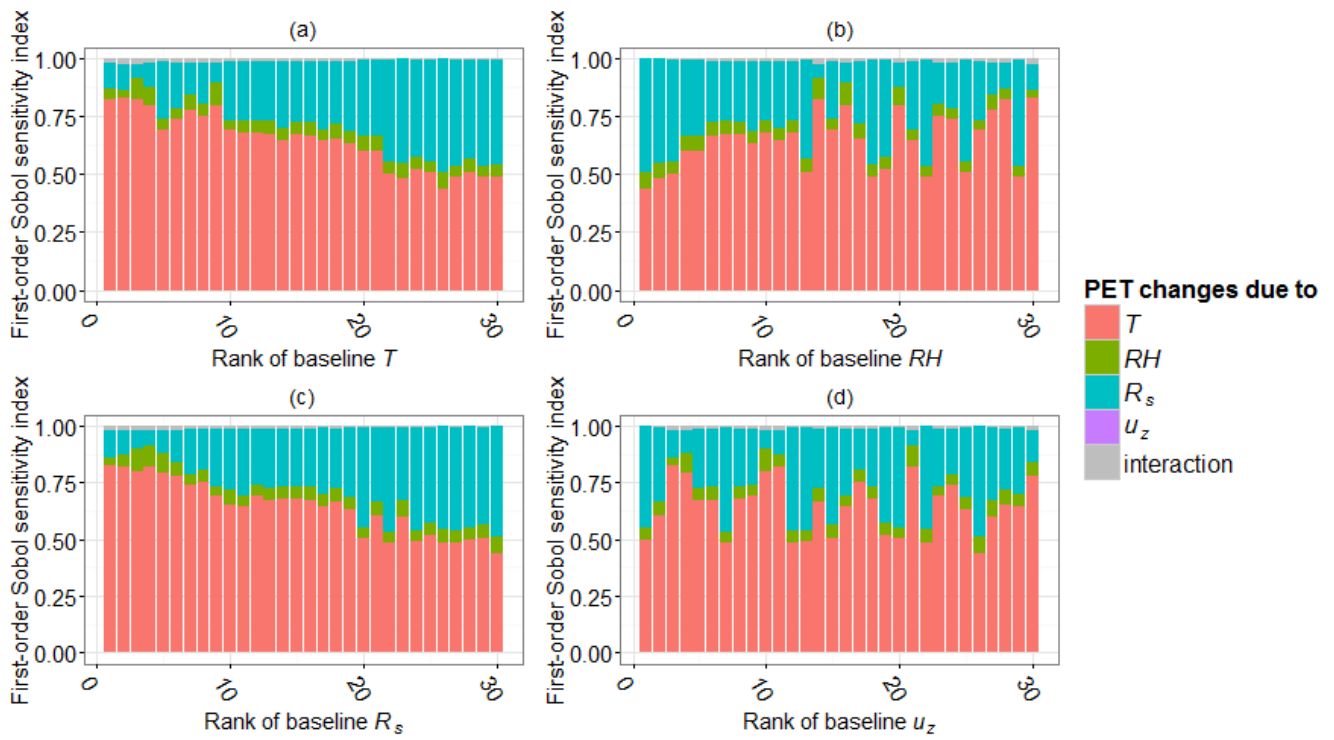
876

877 **Figure 6: Monthly PET responses from the Priestley-Taylor model, plotted against the monthly baseline levels of (a)**
 878 **temperature, (b) relative humidity, (c) solar radiation and (d) wind speed at 30 study sites. Each dashed (solid) line**
 879 **represents the range of all PET responses to the full set of climate perturbations (conditioned on no-change in each**
 880 **climate variable) for a single month at a single location. The corresponding means are represented by the points on**
 881 **the lines. The classification of energy- and water-limited months are based on the corresponding monthly PET/P**
 882 **ratios.**

883



884
 885
 886 **Figure 7: Sobol' first-order sensitivity indices of the Penman-Monteith model for changes in the four climate**
 887 **variables (colored) and their interaction effects (grey), plotted against the ranking of the average level of each climate**
 888 **variable at 30 study sites**
 889



890
 891
 892
 893
 894
 895

Figure 8: Sobol' first-order sensitivity indices of the Priestley-Taylor model for changes in the four climate variables (colored) and their interaction effects (grey), plotted against the ranking of the average level of each climate variable at 30 study sites

Table 1: Names, locations and average climate conditions of the 30 weather stations over the study period (1995-2004).

No.	Study site name	Köppen class ¹	Lat (°S)	Long (°E)	Elev (m)	<i>T</i> (°C)	<i>RH</i> (%)	<i>R_s</i> (MJ m ⁻² day ⁻¹)	<i>u_z</i> (m s ⁻¹)	Annual P (mm)	Annual PET (mm)	Annual PET/P
1	Broome airport	13	-17.95	122.2	7.4	26.37	65.15	21.55	3.684	865	2003	2.317
2	Perth	8	-31.93	116.0	15.4	18.54	61.72	18.95	4.519	721	1751	2.429
3	Albany	4	-34.94	117.8	68	15.08	73.59	15.20	4.382	752	1126	1.498
4	Giles	24	-25.03	128.3	598	22.70	38.40	20.29	4.380	394	2344	5.947
5	Darwin	35	-12.42	130.9	30.4	27.42	69.27	20.33	3.393	1976	1864	0.944
6	Gove	35	-12.27	136.8	51.6	26.29	75.93	19.45	3.500	1607	1660	1.033
7	Tennant Creek	13	-19.64	134.2	375.7	25.73	37.21	21.64	4.759	539	2634	4.886
8	Alice Springs	15	-23.80	133.9	546	21.18	44.53	20.79	2.352	331	1822	5.503
9	Woomera	24	-31.16	136.8	166.6	19.41	46.57	19.40	5.057	151	2153	14.24
10	Ceduna	11	-32.13	133.7	15.3	16.92	62.04	18.20	5.450	266	1723	6.478
11	Adelaide airport	12	-34.95	138.5	2	16.37	63.04	16.91	4.213	454	1410	3.107
12	Adelaide (kent town)	12	-34.92	138.6	48	16.95	61.20	16.88	3.161	569	1372	2.409
13	Loxton	12	-34.44	140.6	30.1	16.50	59.41	17.59	3.250	255	1490	5.847
14	Mount Gambier	4	-37.75	140.8	63	13.45	72.77	14.91	4.460	731	1116	1.526
15	Weipa	41	-12.68	141.9	18	26.87	72.21	19.31	3.271	2154	1782	0.827
16	Cairns	36	-16.87	145.7	3	24.80	73.00	18.98	4.352	1985	1678	0.845
17	Townsville	35	-19.25	146.8	4.3	24.53	69.45	20.27	4.304	1099	1802	1.641
18	Cobar	15	-31.48	145.8	260	19.08	50.64	19.05	2.458	398	1565	3.936
19	Williamstown	9	-32.79	151.8	9	17.84	70.57	16.07	3.927	1145	1309	1.143
20	Sydney	9	-33.94	151.2	6	18.19	67.69	15.97	5.311	1017	1393	1.369
21	Canberra	6	-35.30	149.2	578.4	13.36	65.82	16.86	3.302	590	1226	2.078
22	Wagga Wagga	9	-35.16	147.5	212	15.77	61.78	17.48	3.288	552	1436	2.602
23	Mildura	12	-34.24	142.1	50	17.11	55.62	18.24	3.604	246	1645	6.681
24	East sale	6	-38.12	147.1	4.6	13.77	72.32	14.92	4.062	529	1093	2.067
25	Scottsdale	3	-41.17	147.5	197.5	13.19	70.55	14.23	2.921	931	912	0.980
26	Bicheno	3	-41.87	148.3	11	14.69	66.68	13.69	3.319	690	966	1.401
27	Lake Leake	3	-42.01	147.8	575	9.96	75.40	13.44	3.358	732	774	1.056
28	Hobart	3	-42.83	147.5	4	12.77	65.67	14.04	4.367	483	1097	2.273
29	Strathgordon village	3	-42.77	146.0	322	10.70	77.95	11.65	2.473	2626	699	0.266

30	Flinders Island	3	-40.09	148.0	9	13.54	73.59	14.34	6.399	654	1064	1.626
----	--------------------	---	--------	-------	---	-------	-------	-------	-------	-----	------	-------

898 **Note:**

899 ¹The Köppen classes are presented with their corresponding identifiers from Stern et al. (2000), as: 3. Temperate - no
900 dry season (mild summer); 4. Temperate - distinctly dry (and warm) summer; 6. Temperate - no dry season (warm
901 summer); 8. Temperate - moderately dry winter (hot summer); 9. Temperate - no dry season (hot summer); 11.
902 Grassland - warm (summer drought); 12. Grassland - warm (persistently dry); 13. Grassland - hot (winter drought); 15.
903 Grassland - hot (persistently dry); 24. Desert - hot (persistently dry); 35. Tropical - savanna; 36. Tropical - rainforest
904 (monsoonal); 41 Equatorial - savanna.

905 ² T = temperature, RH = relative humidity, R_s = incoming solar radiation, u_z = wind speed, P = rainfall, PET = potential
906 evapotranspiration calculated using the Penman-Monteith model.

907

908

Table 2: Plausible perturbation bounds for each climate variable relative to their current levels.

Climate variable	Perturbation range
<i>T</i>	0 to +8 °C
<i>RH</i>	-10 % to +10 %
<i>R_s</i>	-10 % to +10 %
<i>u_z</i>	-20 % to +20 %

909

Note: *T* = daily temperature, *RH* = daily relative humidity, *R_s* = daily incoming solar radiation, *u_z* = daily wind speed.

910

911

912 **Table 3: Annual average PET sensitivity to the full set of climate perturbations (as % changes to baseline PET) from**
 913 **the Penman-Monteith and Priestley-Taylor models at the 30 study sites relative to the 1995-2004 baseline. The**
 914 **maximum and minimum sensitivity values from each model are shaded in grey.**

No.	Study site name	Penman-Monteith			Priestley-Taylor		
		Min.	Max.	Avg.	Min.	Max.	Avg.
1	Broome airport	-12.33	39.10	11.16	-9.61	33.75	9.59
2	Perth	-13.20	46.67	13.52	-7.98	34.17	10.62
3	Albany	-15.04	54.67	15.21	-7.28	35.49	11.63
4	Giles	-12.30	37.57	10.68	-7.73	25.83	7.27
5	Darwin	-12.73	39.10	10.92	-9.82	33.84	9.50
6	Gove	-13.10	41.34	11.53	-9.74	33.67	9.61
7	Tennant Creek	-12.28	36.45	10.21	-8.35	26.31	7.09
8	Alice Springs	-10.88	34.00	9.80	-8.00	27.41	7.92
9	Woomera	-12.84	43.48	12.73	-7.48	30.35	9.18
10	Ceduna	-13.97	49.61	14.39	-7.62	33.82	10.67
11	Adelaide airport	-14.47	49.80	14.17	-7.22	34.55	11.09
12	Adelaide (kent town)	-13.10	45.43	13.17	-7.15	33.70	10.78
13	Loxton	-12.55	44.05	12.96	-7.18	33.34	10.67
14	Mount Gambier	-15.33	57.97	16.00	-6.58	35.54	12.02
15	Weipa	-12.42	39.06	10.95	-9.66	32.98	9.36
16	Cairns	-14.80	44.74	12.08	-9.42	33.84	9.73
17	Townsville	-13.77	43.21	12.10	-9.43	34.26	9.90
18	Cobar	-10.62	37.49	11.36	-7.64	31.19	9.49
19	Williamtown	-13.64	47.99	13.68	-7.66	34.11	10.76
20	Sydney	-16.24	53.71	14.46	-7.61	35.24	10.98
21	Canberra	-12.41	46.17	13.85	-6.95	33.24	10.92
22	Wagga Wagga	-13.00	46.34	13.43	-7.09	33.27	10.74
23	Mildura	-12.61	44.50	13.05	-7.24	32.75	10.38
24	East sale	-14.43	53.82	15.34	-6.51	36.32	12.19
25	Scottsdale	-13.64	51.53	15.02	-5.42	40.00	13.47
26	Bicheno	-14.81	52.11	14.87	-4.91	46.38	15.68
27	Lake Leake	-16.06	60.36	16.45	-5.11	36.03	12.84
28	Hobart	-15.97	56.29	15.78	-4.57	50.36	17.77
29	Strathgordon village	-13.08	52.11	15.29	-4.66	33.83	12.35
30	Flinders Island	-18.05	64.07	17.15	-6.19	38.66	13.02
Average		-13.66	47.09	13.38	-7.39	34.47	10.91

915